UNIVERSIDAD DE INVESTIGACIÓN DE TECNOLOGÍA EXPERIMENTAL YACHAY

Escuela de Ciencias Físicas y Nanotecnología

TÍTULO: The complexity of polarization in social dynamics

Trabajo de integración curricular presentado como requisito para la obtención del título de Físico

Autor:

David Mateo Carpio Rivas

Tutor:

PhD. Mario G. Cosenza Miceli

Urcuquí, noviembre del 2023

AUTORÍA

Yo, **David Mateo Carpio Rivas**, con cédula de identidad 0302453980, declaro que las ideas, juicios, valoraciones, interpretaciones, consultas bibliográficas, definiciones y conceptualizaciones expuestas en el presente trabajo; así cómo, los procedimientos y herramientas utilizadas en la investigación, son de absoluta responsabilidad de el/la autora (a) del trabajo de integración curricular. Así mismo, me acojo a los reglamentos internos de la Universidad de Investigación de Tecnología Experimental Yachay.

Urcuquí, noviembre 2023.

_____

David Mateo Carpio Rivas

CI: 0302453980

AUTORIZACIÓN DE PUBLICACIÓN

Yo, **Carpio Rivas David Mateo,** con cédula de identidad 0302453980, cedo a la Universidad de Investigación de Tecnología Experimental Yachay, los derechos de publicación de la presente obra, sin que deba haber un reconocimiento económico por este concepto. Declaro además que el texto del presente trabajo de titulación no podrá ser cedido a ninguna empresa editorial para su publicación u otros fines, sin contar previamente con la autorización escrita de la Universidad.

Asimismo, autorizo a la Universidad que realice la digitalización y publicación de este trabajo de integración curricular en el repositorio virtual, de conformidad a lo dispuesto en el Art. 144 de la Ley Orgánica de Educación Superior

Urcuquí, noviembre del 2023.

_____

David Mateo Carpio Rivas

CI: 0302453980

Dedication

To Elena and Justiniano,

This work is a tribute to your belief in me
and your constant presence by my side.

Mateo Carpio Rivas

Acknowledgements

Abstract

The rise of extreme polarization of opinions in societies is a problem of much interest that has recently been approached in the context of complex systems. In this work, we investigate the dynamics of opinion formation using agent-based models to understand the processes underlying polarization in social networks. To study the dynamics of interactions between agents, we employ the Attraction-Repulsion Agent-Based Model that leads to polarization recently proposed by R. Axelrod and his collaborators. We introduce two different mechanisms for controlling and preventing extreme polarization in this model. First, we study the influence of mass media, considered as an external global field, on opinion formation dynamics. Secondly, we consider an extension of the Attraction-Repulsion Model as a coevolutionary network dynamics, where both the opinions of the agents and their mutual connections vary over time. Our results reveal that, in a social system capable of extreme polarization, mass media messages located around the middle of the opinion spectrum can slow down and even prevent the polarization process. In contrast, extremist messages push agents' opinions toward the opposite extreme, leading to asymmetric polarization within the system. For the coevolutionary model, we found that the rewiring of connections based on the principle of homophily can lead to the emergence of a central-opinion group, thus avoiding polarization in a low-tolerant network.

Keywords: Complex Systems, Opinion Dynamics, Agent-Based Modeling, Polarization, Mass Media, Coevolution.

Resumen

El aumento de la polarización extrema de opiniones en las sociedades es un problema de gran interés que recientemente se ha abordado en el contexto de sistemas complejos. En este trabajo, investigamos la dinámica de la formación de opiniones utilizando modelos basados en agentes para comprender los procesos subyacentes a la polarización en las redes sociales. Para estudiar la dinámica de interacciones entre agentes, empleamos el Modelo de Agentes de Atracción-Repulsión que conduce a la polarización, propuesto recientemente por R. Axelrod y sus colaboradores. En este modelo, introducimos dos mecanismos diferentes para controlar y prevenir la polarización extrema. En primer lugar, estudiamos la influencia de los medios de comunicación masivos, considerados como un campo global externo, en la dinámica de formación de opiniones. En segundo lugar, consideramos una extensión del Modelo de Atracción-Repulsión con una dinámica de red coevolutiva, donde tanto las opiniones de los agentes como sus conexiones mutuas varían con el tiempo. Nuestros resultados muestran que, en un sistema social capaz de polarización extrema, los mensajes de los medios de comunicación ubicados alrededor del punto medio del espectro de opiniones pueden frenar e incluso prevenir el proceso de polarización. Por el contrario, los mensajes extremistas impulsan las opiniones de los agentes hacia el extremo opuesto, lo que lleva a una polarización asimétrica dentro del sistema. Para el modelo coevolutivo, encontramos que el recableado de las conexiones basado en el principio de homofilia puede llevar a la emergencia de un grupo de opinión central, evitando así la polarización en una red con baja tolerancia.

Palabras clave: Sistemas Complejos, Modelos Basados en Agentes, Dinámica de Opiniones, Polarización, Medios de Comunicación, Coevolución.

Contents

List of Figures

List of Tables

Chapter 1

Introduction

In recent years, the study of complex systems has garnered increasing interest, particularly when examining phenomena characterized by collective behavior. Complex systems are systems with multiple interacting components whose collective behavior cannot be simply inferred from the behavior of the components but emerge from its interactions"[1]. These systems show distinctive features, including synchronization, self-organization, adaptive interaction, chaotic behavior, 'fat-tailed' distributions, and emergent behavior[2]. The phenomenon of emergence itself occurs when the non-linear coupling of many elements induces the system's collective behavior, that is, the whole is different from the sum of the parts[3], while self-organization refers to a dynamic process through which a system spontaneously generates complex macroscopic structures and behaviors as time progresses[4]. This contemporary perspective has opened up new routes for exploring challenges beyond the traditional confines of Physics.

Specifically, Statistical Physics offers diverse concepts and methodologies that align closely with the objectives of complex systems science. Both fields share a common aim: understanding the macroscopic characteristics of physical systems through microscopic interactions among their constituent particles. Applications of complex systems extend across various disciplines, including the social sciences, where this field has been called Sociophysics and Computational Social Science. Numerous processes deserve exploration in this context, such as opinion formation, group dynamics, language evolution, pedestrian patterns, migration trends, and cultural dynamics. In particular, opinion formation has been a central topic of interest in social dynamics[5]. The study of agreement or consensus is a key aspect to understand since it is necessary for a social group to reach a shared decision. However, the dynamics of agreement or disagreement in a social group is complex[6]. Two main approaches to model spontaneous consensus are game theory and dynamical opinion formation. A limitation of the first is that due to the unrealistic assumptions about individuals' information access and processing capabilities. For the dynamic approach, we employ the concepts of emergence and self-organization that have been advanced in the field of statistical physics to understand the global consequences of individual adaptive behaviour[7].

In the context of Sociophysics, agent-based modeling is a frequently employed technique for deriving macroscopic states through the interactions of individual agents at the microscopic level. Indeed, we can apply agent-based models (ABM) to understand the emergent behavior of societies by building "artificial societies." An artificial society has

a set of autonomous agents that act in parallel and communicate with each other. This allows us to run virtual experiments by configuring a series of simulations to investigate specific research questions. These simulations involve activating all agents within the system and observing the resulting macro-level behaviors that arise as these agents interact[8].

The rise of extreme polarization of opinions in social groups is a problem of great interest that has recently been approached in the context of complex systems. Agent-based modeling techniques have been applied to investigate the mechanisms underlying the phenomenon of polarization of opinions[9].

1.1 Research Problem

Polarization of opinions is related to the divergence of opinions and the reduction of communication with those holding different points of view[10]. In today's data-rich environment, numerous studies have documented the presence of extreme polarization in real-world scenarios, such as on social media platforms like X (former Twitter)[11] or Facebook[12]. Polarization of opinions can result in adverse outcomes, as evidenced by the democratic erosion in Hungary and the United States, the rise of authoritarianism in Turkey, Nicaragua, and Venezuela[13], or the intensification of political polarization in Ecuador, where state crises and strategic populist maneuvers have significantly contributed to the political divide[14].

Various theoretical models have been proposed to elucidate the processes leading to polarization, with negative influence or repulsion being considered as a mechanism contributing to its emergence[15]. Consequently, once these models have shed light on the polarization process, nowadays, there is a critical need to identify interventions capable of controlling the rise of extreme polarization of opinions in a society.

Motivated by the relevance of the present problem of extreme polarization of opinions and the search for possible control strategies, in this thesis, we investigate mechanisms for controlling or preventing polarization in a social network. To understand the dynamics of interaction that leads to polarization, we employ the Attraction-Repulsion Agent-Based Model recently proposed by the prominent social scientist Robert Axelrod and his collaborators[15].

Specifically, we explore two mechanisms for controlling polarization. First, we study the influence of mass media, considered as an external global field, on opinion formation dynamics. Secondly, we introduce coevolutionary network dynamics as a generalization of the Attraction-Repulsion Model, where both the agent's opinions and their connections vary over time.

1.2 Objectives

1.2.1 General Objective

To investigate mechanisms to control or avoid the emergence of extreme polarization of opinions in a sociophysical model of interacting agents.

1.2.2   Specific Objectives

- Investigate the effects of mass media, incorporated as an external global field, on the polarization of opinions in Axelrod's Attraction-Repulsion Model.

- Generalize Axelrod's Attraction-Repulsion Model by introducing a coevolutionary dynamics where both the agents' opinions and their connections are coupled and can evolve in time.

- Explore the effects of coevolutionary dynamics on the emergence of polarization of opinions.

Through these objectives, we show that Sociophysics can contribute valuable insights and strategies for addressing the challenge of extreme polarization in social networks.

1.3   Overview

This thesis comprises five chapters, organized as follows.

Chapter 2 lays the foundation by introducing key concepts and prior research upon which this project builds. We begin by discussing agent-based models, different kinds of networks, and opinion dynamical models. Then, we focus on the Attraction-Repulsion Model (ARM) proposed by Robert Axelrod[15] for studying polarization. Next, we review how to include an external global field representing mass media in opinion dynamical models. Lastly, we examine the process of extending a model initially focused solely on network dynamics to a coevolutionary model, encompassing both network dynamics and agent interactions.

In Chapter 3, we present our extension of the Attraction-Repulsion Model to include mass media. Mass media is considered an external global field characterized by two parameters: the mass media message position x_M and its intensity B. Then, we investigate the impact of the field in a highly and in a low-tolerant population. We explore their role in the polarization of opinions, the size of the largest cluster, and its difference with the cluster containing the same opinion as the media. We further extend these investigations across various network structures, global, circulant, and small-world networks.

In Chapter 4, we develop the concept of coevolution within the Attraction-Repulsion Model (ARM). This involves simultaneous variations in the actors' states and their connections. To achieve this, we initiate extending the ARM computation from a global to a random network. The coevolutionary model integrates ARM for node dynamics and incorporates the Holme-Newman conditions for the network dynamics. Our in-depth analysis is centered on examining how the rewiring parameter (P_r) influences the system's polarization dynamics.

Chapter 5 serves as the culmination of our research efforts, presenting a comprehensive summary of our findings and drawing meaningful conclusions from our work. Additionally, we offer valuable insights into potential avenues for future research, building upon the models and discoveries presented in this thesis.

Two Appendices containing the computational codes elaborated in Python for our simulations are included at the end of this thesis; the first corresponds to the mass media model, and the second to the coevolutionary network

dynamics.

Simulations are also accessible in video format on the GitHub repositories attached in the Appendices for both the Attraction-Repulsion Model with Mass Media and the Coevolutionary Attraction Repulsion Model.

Chapter 2

Theoretical framework

2.1 Agent-Based Modeling

Agent-based modeling is a novel approach to understanding nature that has emerged from the field of Complex Systems. The fundamental concept behind agent-based models (ABM) is that numerous phenomena in the world can be aptly represented through the utilization of discrete elements or agents, an environment, and an articulation of the interactions between the agents themselves and between the agents and their environment[16]. Then, we can examine how these simple local rules lead to emergent complex patterns and structures. This simulation strategy represents a research methodology that transcends traditional methods of deriving a general theory from empirical data or working from a set of axioms. In ABM, we begin by establishing a set of foundational principles, from which we generate specific data, thereby enabling the formulation of theory[17].

In ABM, agents represent individuals who have been assigned state variables that describe their particular states. At each step of time, the behavior of an agent follows a computational rule[18]. Some states are fixed in time, while others change by interactions with other agents or external factors[19]. For example, in Figure 2.1, the agent i has the state variables T, R, and E, which are fixed in time, while the opinion variable $x_i(t)$ changes in time.

i

$x_i =$ Opinion $E_i =$ Exposure

$T_i =$ Tolerance $R_i =$ Responsiveness
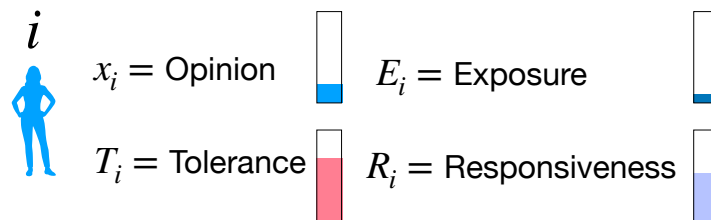
Figure 2.1: State variables of an agent, i.

The environment serves as the background upon which agents interact, and it can take various forms, such as geometric, network-based, or derived from empirical data. In Section 2.2, we review some networks upon which the agents can interact. The agents' actions depend specifically on the phenomenon we are interested in modeling. Examples are shown in Sections 2.3 and 2.4. In these sections, we mention models where the state variable of the nodes, called opinion, changes in time according to some specific social rules.

Indeed, when the action assumptions for the agents align with human behavior, these models become valuable for modeling and simulating social systems. The idea is to build models where the agents are assigned some social properties and then to simulate their interactions. The aim is to address the problem from a lower level to a higher level in the social system[6]. Rather than accurately representing an empirical application as a historical or future event prediction, ABM tries to give us insights about fundamental processes or mechanisms applicable across various social scenarios[17].

2.2 Review of regular and complex networks

We represent a network by a graph $G = (V, E)$ where $V = \{1, 2, \ldots, N\}$ is the set of nodes (or vertices) and E is the set of the m total edges that connects two nodes. We say that node j is a neighbor of node i if i is connected to node j[4]. It is important to note that we can have directed edges in cases where there is an asymmetric relationship from one node to another. Even if node i has an incident edge connecting to node j, this does not imply the existence of an incident edge from node j to node i. Then, we can denote the set of neighbors of i as v_i. Within this context, we can distinguish several graph properties with unique characteristics. One measure is the degree k_i of the node i, which is the number of links connected to the node i[20] or the size of the set v_i. Thus, the average degree of the network is given by

$$\langle k \rangle = \frac{1}{N} \sum_{i=1}^{N} k_i. \tag{2.1}$$

With this characteristic, we can identify regular graphs where all the nodes have the same degree. An example is a global or complete graph where any pair of nodes is connected[4] as we can see in Figure 2.2 (a). In this network, all the agents have degree $k_i = N - 1$, and the mean degree is $\langle k \rangle = (N - 1)/N$. Another example is the ring layout, where node i is connected to nodes $i - 1$ and $i + 1$ considering boundary conditions. This is a one-dimensional network, and it is shown in Figure 2.2 (b). For this network, an agent i has degree $k_i = 2$, so the mean degree is also $\langle k \rangle = 2$. Another network is the one proposed by Erdős and Rényi[21] that considers N nodes and m edges. The m edges are randomly placed among the N nodes, uniformly distributed from all possible edges. Then, the average degree for this network is $\langle k \rangle = 2m/N$. Figure 2.2 (c) shows the outcome of this topology.

We can also characterize a network with the average path length. This parameter measures how long it takes, on average, to go from one node to another, considering all possible pairs of nodes. Another measure is the clustering coefficient. This coefficient measures the extent to which the neighbors of a particular node are interconnected. It assesses the local cohesiveness or clustering of connections around a node. A small-world network is characterized by high local clustering (like regular graphs) and short average path lengths (like random graphs), making it an

essential model for understanding real-world networks [22]. Figure 2.2 (d) represents this more realistic network since real networks are neither random nor completely regular but combine their characteristics.

In a social context, the nodes of a network represent social actors, while the edges, also referred to as ties, represent some form of connection between them, such as friendships [20].

| (a) | (b) |
| (c) | (d) |
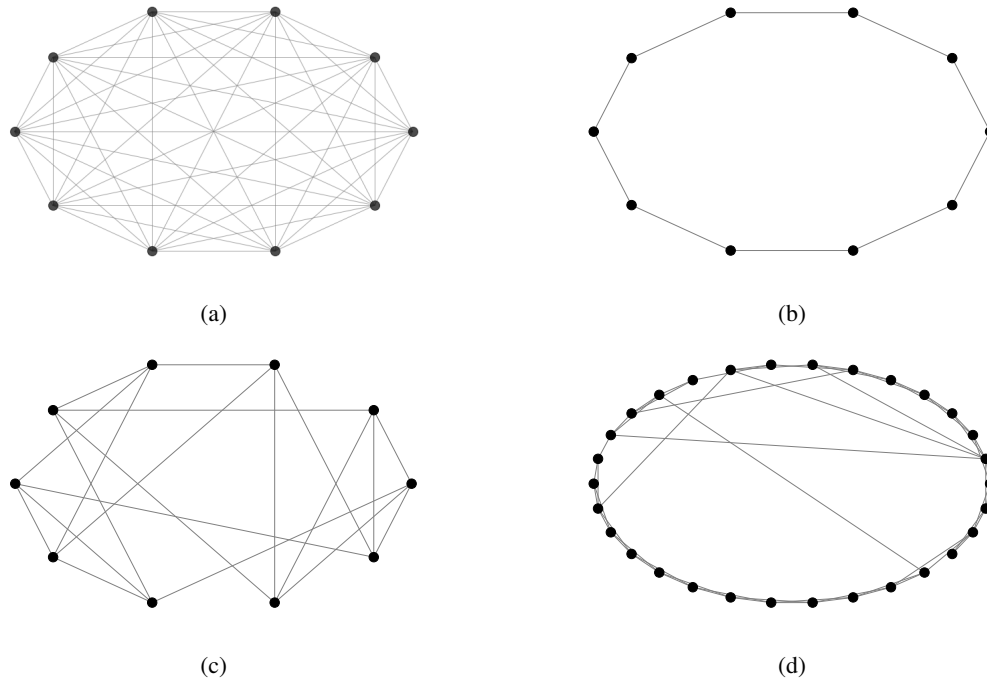
Figure 2.2: Illustrations of different types of network. (a) Global, (b) ring, (c) Erdős–Rényi or random, and (d) small-world networks.

2.3   Opinion dynamics models

One important application of ABM is the study of opinion dynamics in a society. These models have the objective to investigate the dynamical processes involved in the diffusion and evolution of opinions within a population. The actions of the actors in these models are based on principles of social interaction developed in social psychology and sociology [23]. For instance, they incorporate concepts such as imitating the behavior and opinions of others in situations of high uncertainty [24], the persuasive argument theory where interaction partners exchange arguments and convince each other that certain views are more appropriate [25], or the phenomenon of homophily, where individuals tend to interact with those who are similar to them [26].

These sociodynamical models aim to understand the elementary processes determining the transition between

agreement and disagreement[6], or even polarization in a population. A classical opinion model is the voter model[27] where an agent i can have the state variable $x_i = \pm 1$. The state variable of an agent i is updated by choosing a neighbor j randomly and setting $x_i = x_j$. That is, opinion formation is based on imitation. Although it is one of the simplest models, it could lead to emergent patterns[28]. This model has been extended depending on the phenomena we are interested in modeling. For example, including a third option[29], including a set of possible choices[30] or even providing unlimited possible choices in the form of a continuous opinion[31].

Based on the type of variables used for agents, we can categorize opinion dynamics models into two main classes: discrete and continuous models. Discrete models are employed when individuals have a finite set of choices. For instance, in the Dissemination of Culture Model of Axelrod[32], culture is represented as a discrete vector with each component having one of q possible values. In this model, interactions are influenced by the similarity of agents' culture vectors (homophily), and during each interaction, agents tend to adopt one another's cultural components (assimilation).

On the other hand, considering continuous opinions is helpful for cases where the state variable of an agent can vary smoothly from one extreme of the range of possible choices to the other, for example, to model ideological position such as political orientation[6]. One of the first models with these considerations was the one proposed by DeGroot[33]. This model demonstrated how individuals in a network adjust their opinions iteratively, capturing the complex processes involved in reaching a consensus within a social network.

Another example of a continuous model is the one proposed by Deffuant[34]. This model includes a parameter T_i that represents bounded confidence for the agents. By simplicity, the original model considers the same threshold value $T_i = T \; \forall \; i$, which is also constant in time. This means that an agent i with position x_i only interacts with neighbors whose opinion positions fall within the range $[x_i - T, x_i + T]$. The dynamics of the model implies that if the difference between the opinions of agents i and j is inside the bounded limit, they will approach R times its opinion distance. This parameter R is also uniform for all agents, $R_i = R \; \forall \; i$, and remains constant in time. The result of this work was that for values greater than $T \geq 0.5$, the consensus is always obtained independent of the social topology. For values $T < 0.5$, two or more clusters with different opinions in the spectrum $[0-1]$ can emerge during the time evolution. On the other hand, the parameter R controls the convergence speed of the model.

An extension of this bounded confidence model can be obtained if we consider repulsive interactions when their opinion distance is outside the bounded limits of the agent rather than only ignoring them. This consideration is derived from the growing hypothesis that repulsive effects play a role in interactions among individuals with dissimilar opinions[35]. Indeed, evidence of such repulsion dynamics has been observed in real-world systems[36, 37]. R. Axelrod and collaborators proposed a model with this consideration, which we will review in the following section.

2.4 The Attraction-Repulsion Model (ARM)

Wondering if there is a level of ideological polarization above which polarization feeds upon itself to become a runaway process and what policy interventions could prevent such a dangerous positive feedback loop, Axelrold *et al.*[15] proposed an agent-based model that includes both attraction and repulsion interactions between nodes. The

model considers a state variable $x_i(t) \in [0, 1]$ that represents the opinion of the agent i at time t for $i = 1, 2, \ldots N$ where N is the total number of agents. Also, the agents have the variables tolerance T_i, exposure E_i, and responsiveness R_i. This model assumes homogeneity, i.e., $T_i = T$, $E_i = E$ and $R_i = R$, $\forall$ i. Also, these parameters will be considered constant in time.

More precisely, the dynamics of the actors. The first rule is related to the selection of the agents, and it states that agents with similar views tend to interact. In a social context, this rule is based on the principle of social interaction called *homophily*, where individuals prefer to interact with others similar to them. This is represented in Figure 2.3, where interactions between agents with similar opinions (Figure 2.3 (a)) are more frequent than interactions between actors with different points of view (Figure 2.3 (b)). On the other hand, the second rule is related to the dynamics of the agents (represented in Figure 2.4), and it states that interactions between agents with similar points of view reduce their difference (Figure 2.4 (a)). In contrast, interactions between actors with different opinions increase their differences (Figure 2.4 (b)). This negative influence differentiates the model from other agent opinion models.

More precisely, the dynamics of the system is as follows: a randomly selected agent i randomly chooses a neighbor j, and with probability

$$p_{ij} = (1/2)^{d_{ij}/E}, \tag{2.2}$$

an interaction between i and j will happen, where $d_{ij} = \left| x_i - x_j \right|$ is the distance between their opinions and E is a parameter that represents the exposure of the agents to others' opinions. Figure 2.3 (c) shows the behavior of this probability value and the role of the E parameter. We can notice that for low values of E, actors with dissimilar opinions are almost unlikeable of interaction, while for high values of E, this probability increases considerably.

(a)	(b)	(c)
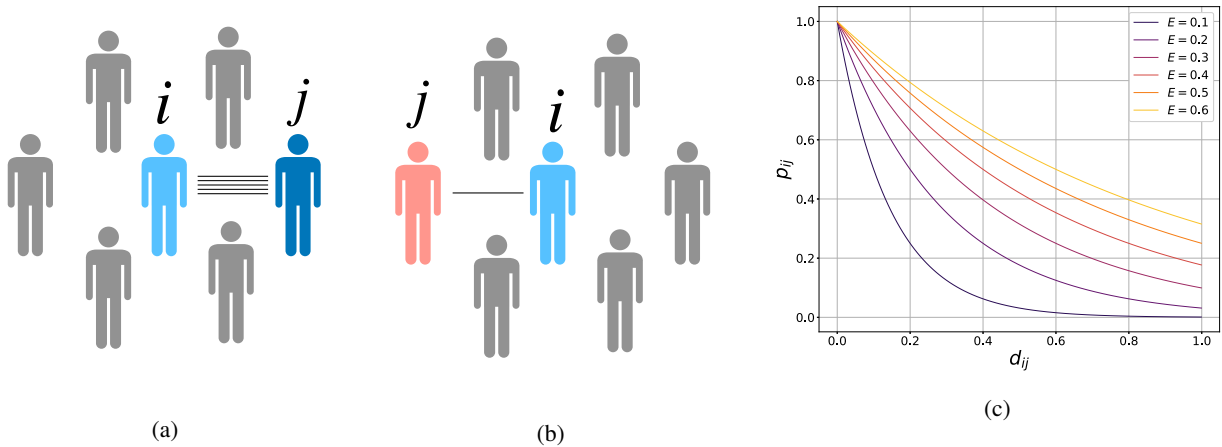
Figure 2.3: Interactions (represented as the number of lines) are more likely between actors with (a) similar opinions than (b) different ones. (c) Behavior of the probability p_{ij} of interaction between agents i and j for different values of exposure E.

Then, if the interaction occurs, we consider the Attraction-Repulsion rule for the dynamics of the agents,

$$x_i(t + \Delta t) = \begin{cases} x_i(t) + R(x_j(t) - x_i(t)), & if \quad \left|x_i - x_j\right| \leq T, \\ x_i(t) - R(x_j(t) - x_i(t)), & if \quad \left|x_i - x_j\right| > T, \end{cases} \quad (2.3)$$

where T is the parameter that measures the tolerance among the population. Notice that in Eq (2.3), the first condition implies that the agent i approaches agent j an amount of R times their distance while the second condition means that agent i moves away from j a number of R times their distance as illustrated in Figure 2.4. Here, R represents the responsiveness of the actors to others' opinions. Since repulsion interactions could lead to opinions leaving the interval $[0, 1]$, we correct this by employing the boundary conditions,

$$if \quad x_i(t + \Delta t) < 0, \quad x_i(t + \Delta t) = 0, \quad (2.4)$$

$$if \quad x_i(t + \Delta t) > 1, \quad x_i(t + \Delta t) = 1. \quad (2.5)$$

.

Here Δt^* representing a time step where an agent is activated.
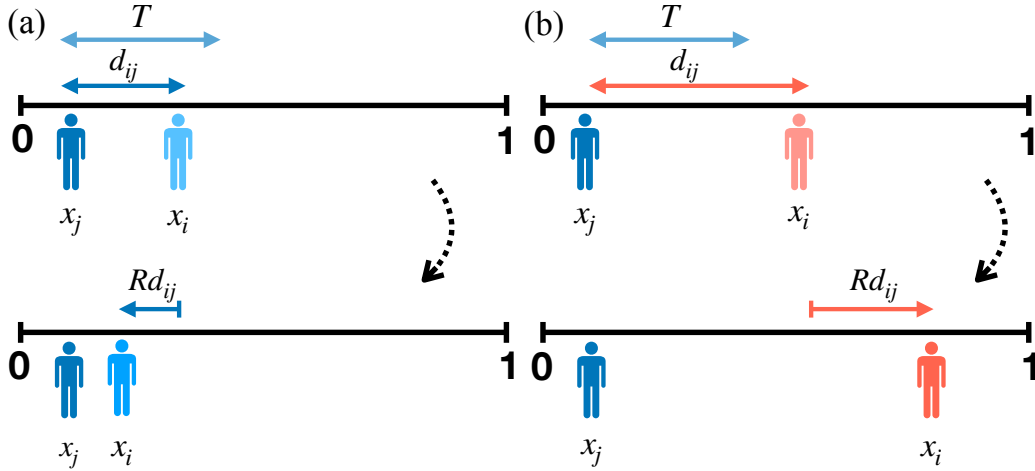
Figure 2.4: Dynamics of the Attraction-Repulsion Model. (a) Interactions between similar actors reduce their difference R times, and (b) interactions between dissimilar actors increase their difference R times.

At each time step Δt, the system follows this iterative algorithm:

1. Randomly chose an active agent i.

2. Randomly chose the source of attention from one of its neighbors j.

3. Calculate the probability of interaction between agents i and j given by $p_{ij} = (1/2)^{d_{ij}/E}$ where $d_{ij} = \left|x_i - x_j\right|$.

---

*There is no obvious calibration of time in the model, but we can use an agent activation, called step, as unit of time.

4. For a successful interaction, if $d_{ij} \leq T$, agent i approach agent j R times d_{ij}. Otherwise agent i moves away agent j R times d_{ij}.

Figure 2.5 shows a flowchart of the model dynamics.
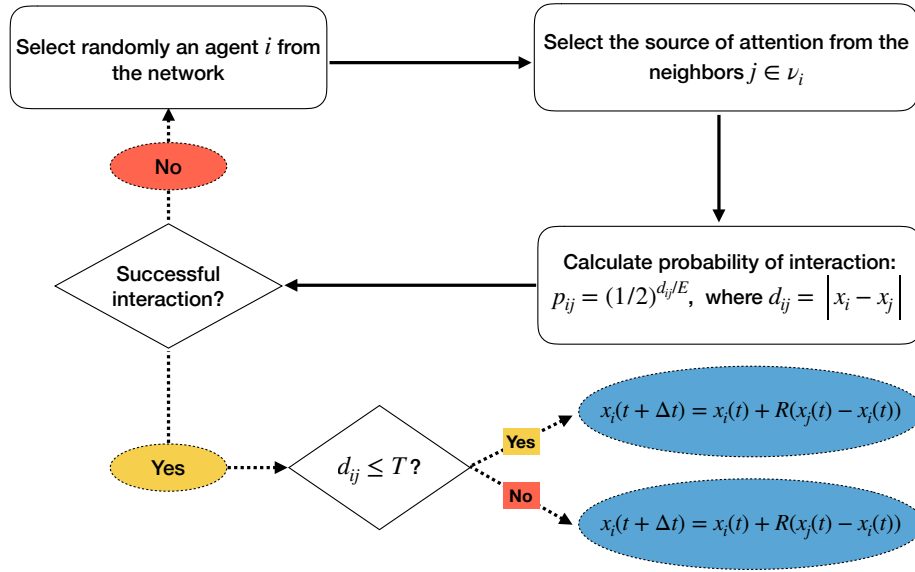
Figure 2.5: Flowchart of the algorithm of the Attraction-Repulsion Model.

Initially, the actors' opinions follow a Gaussian distribution, with mean $\mu_0 = 0.5$ and $\sigma_0 = 0.2$. This assumption is motivated by empirical data, which suggests that a normal distribution is more appropriate for modeling political opinions[38]. This model has been also tested for empirical distribution[39], showing that there is not a meaningful difference between Gaussian and empirical distributions[15]. The measure used to analyze the polarization of the system is the variance. The initial variance given by the initial conditions is $\sigma_0^2 = 0.04$. As the system evolves, the variance can go from $\sigma^2 = 0$, which means convergence to a particular opinion, until $\sigma^2 = 0.25$, which means half of the population is at one extreme and the other half in the opposite extreme.

We then replicated the results of the attraction-repulsion model, but we explored more scenarios in terms of T, R, and E. First, we can identify three scenarios in terms of tolerance, as shown in Figure 2.6 (a). This parameter controls when the effective interactions are attractive or repulsive. As expected, we get the maximum polarization for low tolerance ($T \leq 0.25$) where all the agents have extremist positions. In this case, most interactions are repulsive, leading to polarization. On the other hand, there are more attractive interactions for high enough values of T, and the system converges to a particular position for $T \geq 0.45$. That is, agreement emerges from a high-tolerance population. Finally, for intermediate values such as $T = 0.35$, neither consensus nor extreme polarization is reached; instead, we get a slight variance due to an intermediate majority with some actors at each extreme.

For the responsiveness parameter that modifies how far an actor moves in a successful interaction, whether

this interaction is attractive or repulsive, we can see the effects on the variance as a function of the tolerance after 1.0×10^6 steps[†] in Figure 2.6 (b). Notably, tolerance predominantly determines the transition from polarization to non-polarization, as indicated by the shift from the yellow to the dark zone. On the other hand, the value of R plays a more significant influence on the systems with low tolerance values. Since R controls how far an agent moves, for low values of R, it will be more delayed to reach a complete polarization state in an intolerant population. This explains the smooth transition from a highly polarized to an extremely polarized state as we increase R in populations with low T values.

(a)   (b)
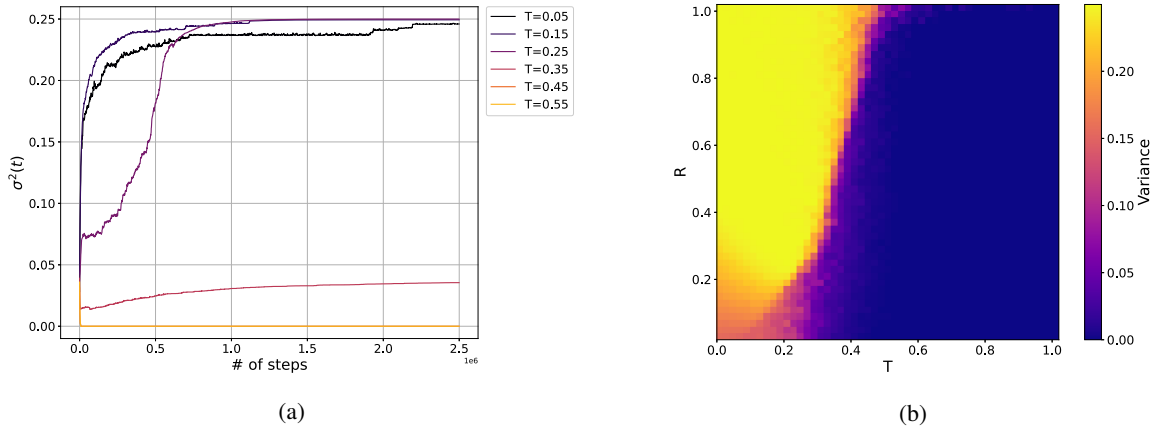
Figure 2.6: (a) Variance as a function of time for different values of tolerance with fixed values $R = 0.25$ and $E = 0.10$. (b) The phase diagram represents responsiveness R and tolerance T with fixed $E = 0.1$ in the polarization of opinions given by the variance. The results were obtained after 1.0×10^6 steps, averaging over 20 iterations for each (T, R) pair in a network of $N = 100$ agents. Yellow means extreme polarization, while dark blue means convergence to a single opinion. The results are based on replicating Axelrod's ARM model[15], incorporating a wider range of R and T values in the phase diagram.

For the exposure, the parameter that measures if actors are willing to listen to distant or similar opinions, simulations show that low values of E help to prevent polarization. In contrast, high values increase the polarization of the system. This is supported by the fact that when the population is considerably intolerant, most interactions are repulsive, and increasing exposure only makes these interactions more frequent. This is shown in Figure 2.7 (a), where it is possible to see how the variance evolves in time for a fixed value of tolerance ($T = 0.3$) for different values of E. Here low exposure values ($E \leq 0.1$) reach lower variance values than high values ($E \geq 0.15$). The explanation is that increasing exposure only makes repulsive interactions more recurrent for a given low-tolerant system.

This result is corroborated in the phase diagram (E, T) shown in Figure 2.7 (b), where we can understand in a more general way the role of the exposure in the model. Again, the parameter T dominates the outcome, especially for high values ($T \geq 0.40$) where the population reaches consensus. In the region for values $0.25 \leq T < 0.40$, we

---

[†]As an example, if an agent becomes active once a day, then one day would correspond to N time steps. Therefore, with $N = 100$ agents, we would have 100 steps per day and 36500 steps in a year. Consequently, 1.0×10^6 steps would be equivalent to over 27 years.

reach a transition region between consensus and extreme polarization with intermediate polarization values. Finally, for the region of intolerant agents ($T \leq 0.25$), we see that high exposure values always lead to extreme polarization, while for values $E \leq 0.1$, it is possible to reduce polarization.

(a)   (b)
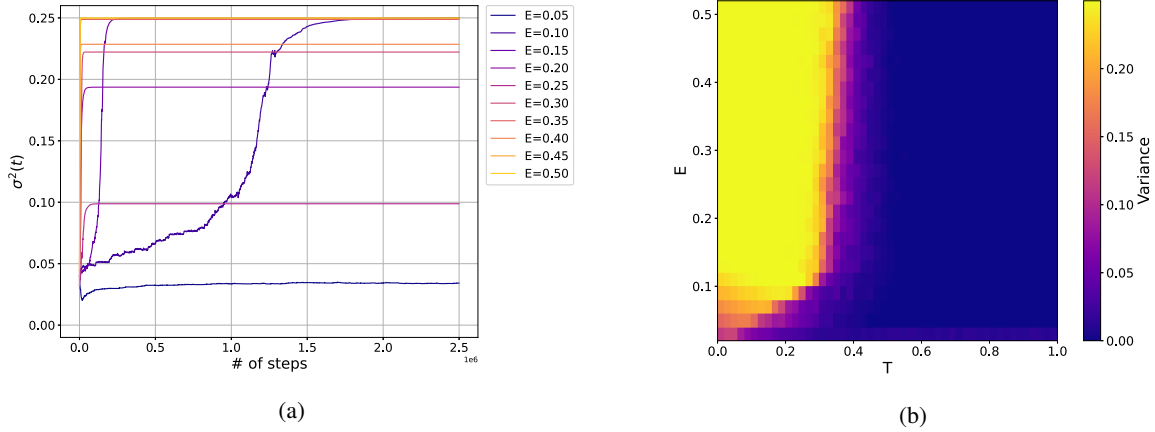
Figure 2.7: (a) Variance as a function of time for different exposure values and with fixed values $R = 0.25$ and $T = 0.25$. (b) The phase diagram represents exposure E and tolerance T with fixed $R = 0.25$ in the polarization of opinions given by the variance. The results were obtained after 2.0×10^6 steps by averaging over 20 iterations for each (T, E) pair in a network of $N = 100$ agents. The yellow color means extreme polarization, while the dark blue means convergence. The results are based on replicating Axelrod's ARM model[15], incorporating a wider range of E and T values in the phase diagram.

In summary, this model is based on two rules: one for the selection of the interaction of the agents and the other for the dynamics of the interaction. The main contribution is the addition of repulsion, which is usually forgotten in polarization models. Similar to Deffuant's model[31], the system tends to converge to a singular opinion for a high value of tolerance ($T \geq 0.40$) regardless of the values of E and R. Interesting results arise when we explore the system for lower values of T. One remarkable result occurs when we have more repulsive interactions than attractive ones. In this region of intolerant agents, high values of E lead to extreme polarization, while R makes these repulsive interactions more pronounced, leading to extreme polarization more easily. On the other hand, low values of E prevent these repulsive interactions, while low values of R delay the polarization.

We were able to reproduce the original Axelrold *et. al.* results from scratch and with another programming methodology[‡]. This replication procedure is a fundamental stage in the process of performing simulations in the computer social sciences[17]. Also, we improve the resolution in the results in the phase diagrams (T, R) and (T, E) to calculate the final state variance. We increase the grids from (20×20) and (20×10) to (50×50) and (50×25), respectively. At the end, we corroborate the results obtained by Axelrold. *et al.* with ours.

With these results, Axelrod *et al.* propose extensions to the model, such as geography modifications or considering

---

[‡]For performing the simulations, we incorporate Python's library NetworkX.

significant social influence with unchangeable opinions. The first extension could be achievable by changing the network where the nodes interact. Notice that in the original model, all the agents have a certain probability of interacting with each other. That is, all are connected in a global network. However, we can consider a new kind of network. Also, we can vary the connection of the agents over time. For the second extension, we can consider an external global field acting over all the agents analogically to a mass media. So, let us briefly comment on these kinds of models.

2.5   Models of social dynamics with mass media

The dynamics of opinions of social agents in a network does not always depend on the agent-agent interaction, but it could also be affected by external factors such as an external global field. Indeed, we can distinguish both local and global interactions in dynamical systems. In local interactions, an individual is affected by the elements from its local environment while in global interactions, all the individuals are affected by a common influence that is acting in the whole system. In a social context, adding a field to the system can be understood as mass media and the information it gives to the system as propaganda. The aim of including mass media is to understand under what condition propaganda changes the opinion dynamics of the system[40]. Indeed, the role of the media in the polarization of opinions has been extensively discussed, especially for political opinions[41, 42].

Mass media is mainly characterized by the message it gives and its intensity (or frequency)[43]. It can be distinguished in various ways. Spatially, it may be either uniform, representing global media, or non-uniform, representing local media. Additionally, media can be categorized based on whether the message remains constant or changes over time. If it is constant in time, it can be understood as specific advertising imposed by the media. This case corresponds to a driven spatiotemporal dynamical system. On the other hand, if the message conveys information obtained from the system, it could be understood as an autonomous dynamical system. A way to update the message is by choosing the most abundant position in the population. This kind of autonomous field could be understood as a media that takes the position of the trending topic[44].

Several works have investigated the role of mass media on different opinion dynamical models. For example, there are studies of including media in Axelrold's cultural model[43–45] or in the Deffuant model[40, 46].

2.6   Models of coevolutionary dynamics

The models that we have described in this chapter are developed in static networks where only agents' opinions, not links between them, change over time. We can distinguish between *the dynamics ON the network* (as in the ARM model) and the *dynamics OF the network*. In the first one, each node of the network represents a dynamical system while in the second one, the topology of the network is treated as a dynamical system changing in time according to specific rules[47]. Many real systems lie between these two cases, where both state variables of the nodes and their connections vary on time. By combining these notions, we encounter networks whose connections adaptively change according to their states. As a result, a dynamic interplay emerges between the nodes' states and the network's topology, resulting in a feedback effect between them[48].

A coevolution model consists of three main components. First, the agents' dynamics describes how the actors' state variable will change. Some examples were described in Section 2.3 and Section 2.4, like the voter, bounded confidence, or attraction-repulsion models.

Second, we have the dynamics of the connections among the agents. This dynamics is based on a rewiring process that involves two simple actions: disconnection and connection between nodes[49]. The disconnections can be seen as a repulsion between agents and are characterized by a parameter d that represents the probability that two nodes with similar states get disconnected. Thus, the probability that two nodes with different states disconnect will be $1 - d$. On the other hand, connections can be seen as attractions between nodes and they are determined by the parameter r, representing the probability that two similar nodes will create a link. So, $1 - r$ will be the probability that two nodes with different states create a new link.

It is possible to construct a phase plane for (d, r) that includes all possible rewiring processes consisting of disconnection and connection[49]. Figure 2.8 represents this phase plane, where we can identify regions of homophily and heterophily. Maximum homophily is achieved at the values $(d, r) = (0, 1)$ where an agent disconnects from an opposite and connects to a similar. On the other hand, maximum heterophily is reached at $(d, r) = (1, 0)$, implying disconnection from similar individuals and connection to dissimilar ones. The transition from heterophily to homophily can be observed by following the arrow in the figure. In this transition, we can have, for example, values of $(d, r) = (0.5, 0.5)$, which means that connections and disconnections are random. Other well-used criteria for d and r are the Holme-Newman condtions[30], which correspond to values $(d, r) = (0.5, 0.5)$ meaning that disconnections are random, but connections are created with the similar ones. Holme-Newman conditions fall within the homophily region.
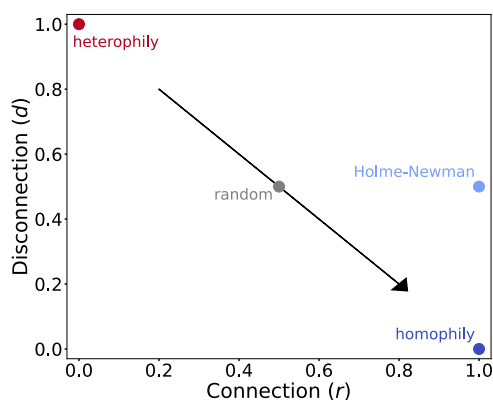
Figure 2.8: A specific adaptive rewiring process can be characterized by two values, r and d, which correspond to a point in the plane (d, r). The point $(0, 1)$ corresponds to total heterophily while the point $(1, 0)$ represents complete homophily. Additionally, point $(0.5, 0.5)$ means that both connections and disconnections are random, while point $(1, 0.5)$ implies that disconnections are random, but connections are created with similar ones. The arrow shows the transition between heterophily and homophily along the diagonal $d = 1 - r$.

The last component for coevolutive models involves a functional relation $P_c = f(P_r)$ between the probability of

applying rewiring, P_r, and the probability that the node state changes, P_c [49]. A simple and very common function is $P_c = 1 - P_r$. The main role of these parameters is to control the rate at which the dynamical processes occur. The competition between their time-scales can lead to a phase transition and directly influence the system's emergent behavior. For example, for a system whose node dynamics leads to consensus, we can expect to reach a single network with all the agents in the same state for low values of P_r. Contrary, for high P_r values, the rewiring process can break the network into different components that will separately reach consensus [6]. These two topological outcomes are separated by a critical value P_r^*.

Coevolutionary dynamical systems or adaptive networks have been studied in several social dynamics and opinion formation models by mixing different node and topology dynamics criteria. An example is the coevolution extension of a non-linear voter model [50] or of the Deffunat model [51, 52].

Chapter 3

Non-trivial effects of mass media on polarization of opinions

3.1 The Attraction-Repulsion Model with Mass Media

We base this chapter on the ARM presented in Section 2.4, where we introduce mass media, labeled as M, as an external global field similar to previous works[43, 45]. The media is characterized by its opinion position x_M with a given value in the spectrum $[0, 1]$. This opinion position is unchangeable over time, so we have that $x_M = constant$. We can understand the media as a driven force acting over a network of N agents $\{i = 1, 2, \ldots, N\}$, which represent social actors. Then, the state variable x_M is the media's opinion, message, or advertising transmitted to the network. The external global field is uniform across the networks since it acts over all the nodes with the same intensity. The strength of the media's influence is characterized by the parameter B, which represents the probability of an agent i considering the media as the source of attention. Here, B takes values within the range $[0, 1]$.

In the model, each agent i has a set of neighbors v_i unchangeable in time. Also, each actor i has a state variable $x_i(t) \in [0, 1]$ representing its opinion on a continuous spectrum at time t. At the beginning, the agents have an initial opinion $x_i(t = 0)$ in such a way that all of them follow a Gaussian distribution between 0 and 1 with a mean of $\mu_0 = 0.5$ and a standard deviation of $\sigma_0 = 0.2$ (for an explanation behind these initial conditions, refer to Section 2.4). For a more illustrative image of the system, the action of the media on the actors is represented in Figure 3.1. It is important to notice that the directional arrows originating from the media and reaching the agents indicate that the media influences the actors' opinion states, but not the other way around. This represents a non-autonomous system.

The agents' opinions evolve according to the dynamics of the model. This dynamic process starts by randomly choosing an agent i. The second step, which is the process of choosing the source of attention, includes the presence of the external global field. The source of attention for an agent i with probability B will be $j = M$ (the media), and with probability $1 - B$, it will be $j = k$ such that $k \in v_i$ (a neighbor of i). This means that either a neighbor or the external field could influence the opinion of an agent i. In the limit $B \rightarrow 0$, the social actor only interacts with its
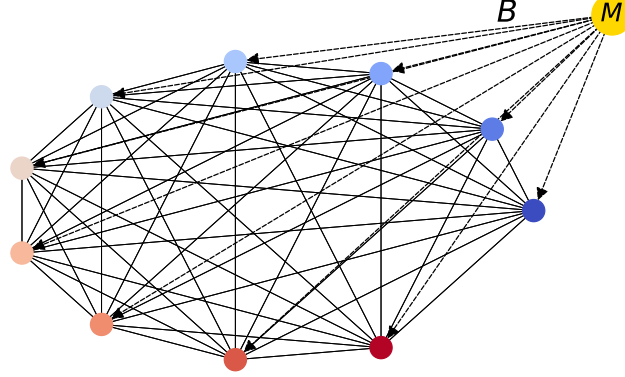
Figure 3.1: The diagram illustrates the mass media, denoted as M, acting with an intensity B on a fully connected network. The colors on the diagram characterize the opinions held by the agents. The arrows pointing from the media towards the agents signify that the advertising media exclusively influences the agents rather than the agents influencing the media.

neighbors. In the opposite limit, $B \to 1$, all the agents' interactions occur with the media.

Once the source of attention is selected, we calculate the probability that the interaction occurs, which is given by

$$p_{ij} = (1/2)^{d_{ij}/E}, \tag{3.1}$$

where $d_{ij} = |x_i(t) - x_j(t)|$ is the distance between the opinions, and E is a parameter that represents the exposure of the agents to others opinion. When $j = M$, this probability becomes in

$$p_{iM} = (1/2)^{d_{iM}/E}, \quad d_{iM} = |x_i - x_M|. \tag{3.2}$$

We can notice that although the probability B that the media is the source of attention is the same for all the actors, the probability of a successful interaction is greater for those near the media position. This agrees with what Robertson *et al.*[53] found where people's actions tend more to interact with their partisan news than the platform's algorithmic suggestions. Then, if the interaction does not occur, we return to the first step. On the other hand, if there is a successful interaction, we consider the following attraction-repulsion rule for the dynamics of node i,

$$x_i(t + \Delta t) = \begin{cases} x_i(t) + R(x_j(t) - x_i(t)), & if \quad |x_i - x_j| \le T, \\ x_i(t) - R(x_j(t) - x_i(t)), & if \quad |x_i - x_j| > T, \end{cases} \tag{3.3}$$

where $j \in v_i$ or $j = M$. In this equation, T is the parameter that measures the tolerance among the population, and R represents the responsiveness of the actors to others' opinions. Notice that the first condition in Eq. (3.3) implies that the agent i approaches j a number of R times their distance if their opinions distance is less than a threshold value

T, while the second condition means that agent i moves away j an amount of R times their distance if the distance is outside the threshold. This implies that when $j = M$, the dynamics of the agent i will be

$$x_i(t + \Delta t) = \begin{cases} x_i(t) + R(x_M(t) - x_i(t)), & if \quad |x_i - x_M| \leq T, \\ x_i(t) - R(x_M(t) - x_i(t)), & if \quad |x_i - x_M| > T. \end{cases} \tag{3.4}$$

Therefore, the media could have attractive or repulsive effects on the agent i. The fact that the media could have repulsive effects on actors in opposite positions than the media agrees with what Bail *et al.*[37] found, where interactions between Twitter users with contrary political views increased their beliefs rather than convinced them.

In summary, the dynamics of the system follows this iterative algorithm:

1. Randomly chose an active agent i.

2. Chose the source of attention j with probability B to be the mass media and with probability $(1 - B)$ to be one of the neighbors of i.

3. Calculate the probability of interaction between i and j given by $p_{ij} = (1/2)^{d_{ij}/E}$ where $d_{ij} = |x_i - x_j|$.

4. For a successful interaction, if $d_{ij} \leq T$, agent i approach j an amount of R times d_{ij}. Otherwise, agent i moves away agent j a number of R times d_{ij}.

Figure 3.2 shows a flowchart of the dynamics for our model.
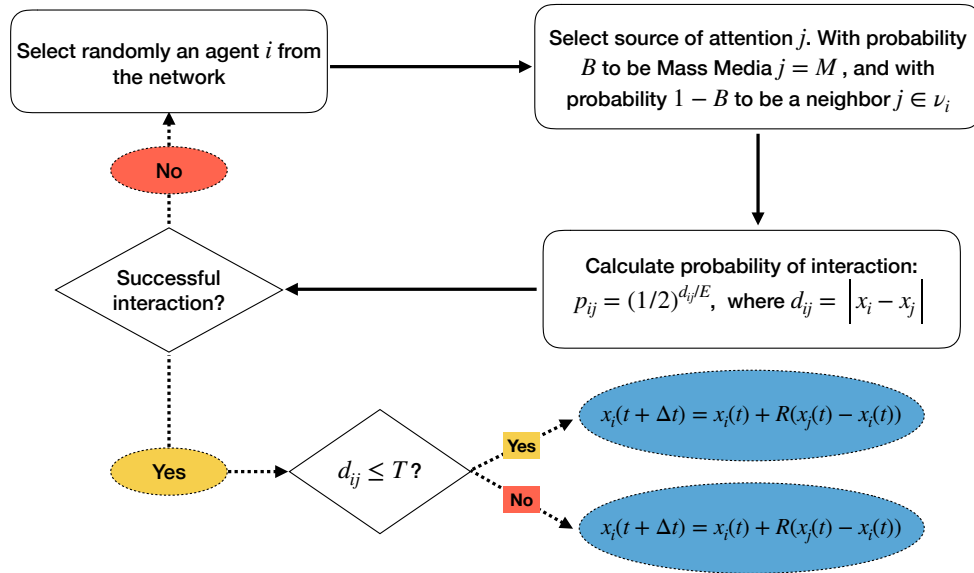
Figure 3.2: Flowchart of the algorithm of the Attraction-Repulsion Model including mass media.

   Our source code for this model can be found in Appendix A. This code includes a timer to monitor the time expended for each simulation. Due to the probabilistic nature of the model, the duration of a full simulation may vary based on the parameters used*. On average, the program processes around 8000 steps per second. For instance, a complete simulation of 2×10^6 steps typically takes approximately 4 minutes, with some variability (± 1 minute).

   All the parameters that intervene in the model dynamics are summarized in Table 3.1. In our pursuit of preventing polarization, we configure the parameters to ensure that without media intervention, the system would tend toward a polarized state. Specifically, we set $R = 0.25$, $E = 0.1$, and $T = 0.25$ in the model discussed in Section 2.4. As illustrated in Figure 2.6 and Figure 2.7, these parameter values position the model just before the transition region between polarization and consensus. Additionally, we examine the system for the parameters $R = 0.25$, $E = 0.1$, and $T = 0.40$, where the model is already located within the consensus region.

Parameter	Symbol	Meaning	Default Value
Mass media message	x_M	Opinion of the mass media	$[0-1]$
Mass Media Intensity	B	Probability of the media to be the source of attention	$[0-1]$
Tolerance	T	Distance within interactions are attractive and beyond are repulsive	0.25 & 0.40
Responsiveness	R	The fractional distance an actor's ideological position moves as a result of an interaction	0.25
Exposure	E	The degree to which actors interact with dissimilar points of view expressed as the halving distance	0.1
Number of Agents	N	Actor that belong to the network	100
Initial Mean and Standard Deviation	μ_0, σ_0	Characterized the initial distribution of the agents opinion's	0.5, 0,2

Table 3.1: Parameters used in the Attraction-Repulsion Model including mass media.

   Once we have described the dynamics of the model, let us introduce the statistical parameters that will help us to characterize the system both during the time evolution of the agents and the asymptotic behavior.

3.2   Statistical parameters

To measure the polarization, we employ the variance of the system $\sigma^2(t)$, defined as the square of the standard deviation. It is given by

$$\sigma^2(t) = \frac{1}{N}\left(\sum_{i=1}^{N}(x_i(t) - \mu(t))^2\right), \tag{3.5}$$

---

*Systems with less frequent successful interaction expends less time.

where $\mu(t)$ is the mean value of the opinion attribute of the N agents at time t. Maximum polarization is reached when $\sigma^2 = 0.25$, that is, exactly half of the population opinions in one extreme, and the other half of opinions located in the other extreme. Minimum polarization occurs when $\sigma^2 = 0$. This happens when all the opinions converge to a single point, so we call this state a complete consensus. Also, we study the system's behavior after a considerable pass of time τ to ensure that we are in a more stable state without abrupt changes in the mean values. For this reason, we use the averaged standard deviation over a long time t_f* after τ transients. It is given by

$$\overline{\sigma^2} = \frac{1}{t_f - \tau} \sum_{t=\tau}^{t_f} \sigma^2(t). \tag{3.6}$$

Since we are treating stochastic components, we can have anomalous behavior if we run the simulation only once. So, to ensure we have characterized the system correctly, we have to run the model several times [16]. Thus, we consider $\langle \sigma^2 \rangle$ as the averaged variance over n different realizations of a simulation

$$\langle \sigma^2 \rangle = \frac{1}{n} \sum_{i=1}^{n} \overline{\sigma_i^2}. \tag{3.7}$$

We call a cluster s_ξ to the set of elements that share the same state. We use the criteria of the same state for the nodes if their state variables belong to the same interval I_ξ of size ϵ,

$$\epsilon = \frac{1}{K}. \tag{3.8}$$

where K [†] is the total number of clusters in the range $[0, 1]$.

Then, the set of elements that correspond to a cluster s_ξ is

$$s_\xi = \left\{ x_i \in [0, 1] : x_i \in I_\xi, \quad i \in \{1, 2, \ldots, N\}, \quad \xi \in \{1, 2, \ldots, K\} \right\}, \tag{3.9}$$

where N is the total number of nodes. In this way, the normalized size of the set of elements belonging to a cluster s_ξ at time t will be

$$S_\xi(t) = \frac{1}{N} |s_\xi|. \tag{3.10}$$

In this context, we use $S_{max}(t)$ as the normalized size of the largest cluster at time t given by:

$$S_{max}(t) = \max \{S_\xi(t), \quad \xi \in \{1, 2, \ldots, K\}\}. \tag{3.11}$$

If the normalized quantity $S_{max}(t)$ is one, the system reaches consensus in a single point. On the other hand, if this quantity tends to zero, the system has diverse opinions. We can define the averaged normalized largest cluster of the system over a long time t_f after τ transients given by

$$\overline{S_{max}} = \frac{1}{t_f - \tau} \sum_{t=\tau}^{t_f} S_{max}(t), \tag{3.12}$$

---

*In this chapter, to measure the final state, we use a total of 2.0×10^6 steps.

†In this work, we set $K = 50$ different clusters. We made this choice because it provides a fine-grained view that allows us to observe meaningful distributions without encountering visibility issues. Additionally, we believe that this quantity effectively covers a wide range of possible clusters that can form in the opinion spectrum.

and the averaged over n realizations of the experiment will be

$$\langle S_{max} \rangle = \frac{1}{n} \sum_{i=1}^{n} \overline{S_{max}^i}. \tag{3.13}$$

Also, we use the quantity $S_M(t)$ as the normalized size of the set of agents possessing the same state that the field at time t. Then, we define the quantity

$$\Delta_M = S_{max}(t) - S_M(t), \tag{3.14}$$

as the difference in normalized sizes between the largest cluster and the cluster containing the media. The averaged quantity over a long time t_f after τ transients will by

$$\overline{\Delta_M} = \frac{1}{t_f - \tau} \sum_{t=\tau}^{t_f} \Delta_M(t). \tag{3.15}$$

We then define the difference of sizes between the largest cluster and the cluster containing the media averaged over n realizations as

$$\langle \Delta_M \rangle = \frac{1}{n} \sum_{i=1}^{n} \overline{\Delta_M^i}. \tag{3.16}$$

If this quantity equals zero, it implies that the largest cluster contains the same position as the media. On the other hand, if this quantity is equal to the size of the largest cluster, any actor follows the position of the media. For better clarity, Table 3.2 summarizes the statistical parameters used to analyze the system.

Parameter	Symbol	Meaning	Values range
Instantaneous variance	$\sigma^2(t)$	Measure polarization at time t	$[0 - 0.25]$
Averaged variance over realizations	$\langle \sigma^2 \rangle$	Measure polarization over n realizations of the same experiment	$[0 - 0.25]$
Instantaneous size of the largest cluster	$S_{max}(t)$	Measure the size of the largest cluster with the same opinion at time t	$[0\text{-}1]$
Averaged size of the largest cluster over realizations	$\langle S_{max} \rangle$	Measure the size of the largest cluster over n realizations of an experiment	$[0\text{-}1]$
The size difference between the largest cluster and the cluster containing the media at time t	$\Delta_M(t)$	Measure the difference between the largest cluster and the cluster with the same opinion that the media at time t	$[0\text{-}1]$
Averaged size difference between the largest cluster and the cluster containing the media over realizations	$\langle \Delta_M \rangle$	Measure the size of the largest cluster and the cluster with the same opinion that the media over n realizations of an experiment	$[0\text{-}1]$

Table 3.2: Statistical parameters used for studying the Attraction-Repulsion Model including mass media.

3.3   Results for low tolerant population

For this section, the parameter values of the system were chosen so that, without applying the field, it would evolve to a state just before the transition point between polarized and non-polarized systems (refer to Figure 2.6). The system is characterized by the default parameters $T = 0.25$, $R = 0.25$, and $E = 0.10$, as shown in Table 3.1. In fact, without considering the field, the system exhibits a high degree of polarization $\langle \sigma^2 \rangle = 0.245$. We then investigate the impact of varying both x_M and B on the system's dynamics.

3.3.1   Global network

We started studying a global network where all nodes are connected, so each agent has $N - 1$ neighbors. Within this network, all actors possess a certain probability of interaction with each other. Also, all the nodes can interact with the field, as it was mentioned.

Figure 3.3 illustrates different population snapshots at various time points. Each column corresponds to different B values, and the rows to different time steps. The colors of the bins represent the opinion position that ranges from zero (blue) to one (red). The yellow represents the cluster with the same opinion as the media. Figure 3.3 (a) shows the evolution of the system without applying the field ($B = 0.00$) (from up to down). We corroborate that at the final state after 2.0×10^6 steps, half of the population aligns with one extreme viewpoint while the other half adheres to the opposing perspective. The system reaches extreme polarization, as expected. However, patterns emerge as we introduce the field's influence.

Our initial focus was analyzing scenarios where the media holds a central position, with $x_M = 0.50$ while changing the values of B. For instance, when $B = 0.10$ (Figure 3.3 (b)), initially, a majority of agents align with the media message, and there are some actors at each extreme. Yet, over time, a significant portion of the agents following the media gradually adopt the extreme positions, culminating in complete polarization after 2.0×10^6 steps. Similarly, when we examine the case of $B = 0.50$ (Figure 3.3 (c)), we observe a similar trend. In the early stages, a substantial fraction of agents follow the media's message, but as time progresses, some of them go to extreme positions. Nonetheless, the media is strong enough to retain many actors aligned with its position for an extended duration. These results show us that the field can attract the actors' opinions, especially for short periods of time. However, it loses attraction as time goes on.

To analyze the temporal evolution of polarization, we can examine the agents' behavior by considering the variance of the system over time. In Figure 3.4 (a), we can see that without the intervention of the field ($B = 0$), the system reaches maximum polarization after about 1.0×10^6 steps. However, upon introducing the field, the variance curve begins to flatten. We see that for $B = 0.20$, the maximum polarization is reached after more than 2.0×10^6 steps, while for higher values, the system does not reach this extreme state even after 2.5×10^6 steps.

Also, Figure 3.4 (b) shows the behavior of the difference between the largest cluster and the cluster with the same opinion that the media over time. When we apply the field, we see that the group with the same opinion as the media becomes the largest cluster. Nevertheless, there comes a point where this cluster is no longer the largest. This shift occurs later in time as we increase the value of B, and it becomes negligible for high field intensities. For example,
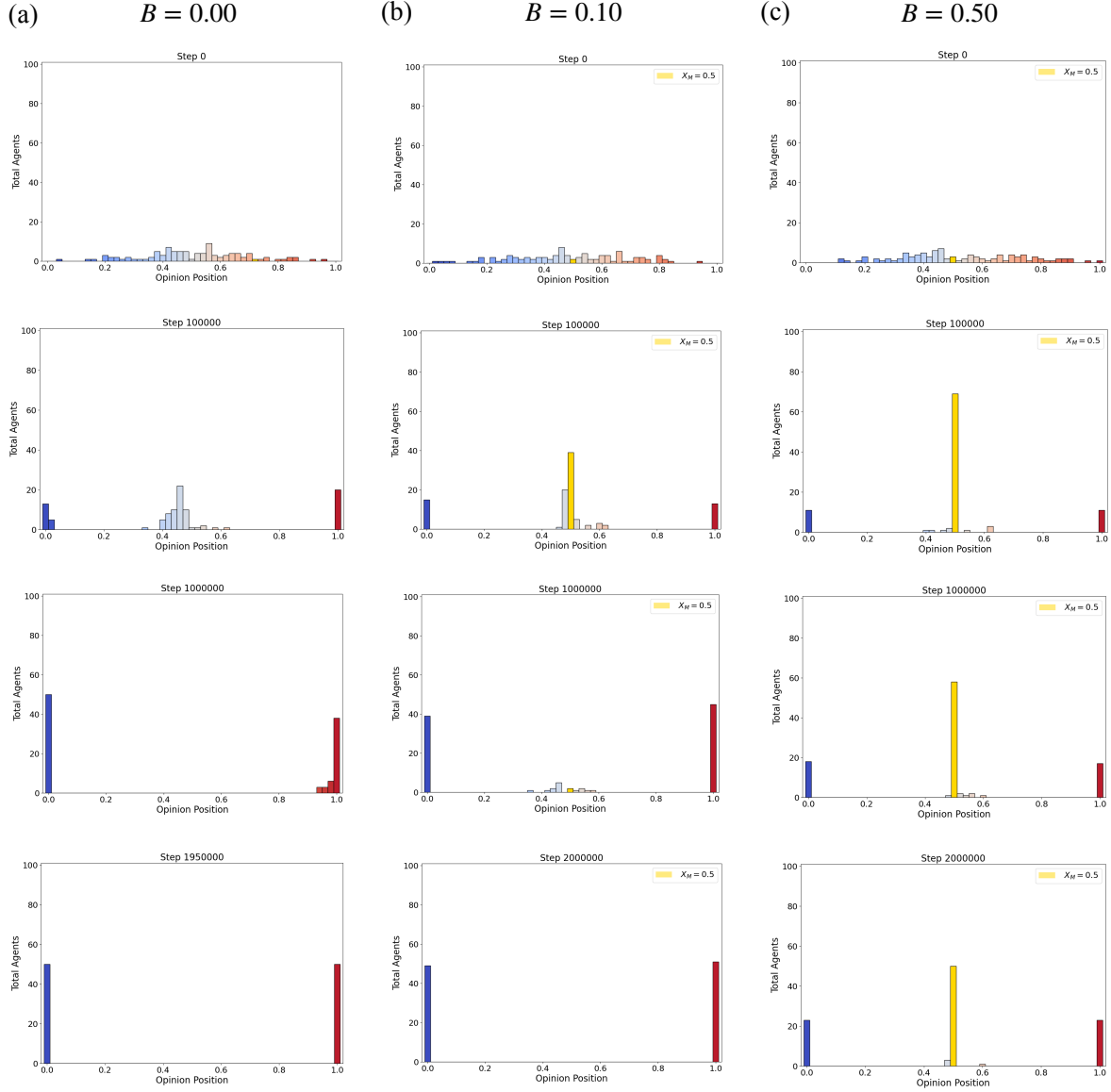
Figure 3.3: Snapshots of the system's time evolution including mass media with central message $x_M = 0.5$. Each column represents a different intensity field B, (a) $B = 0.00$, (b) $B = 0.10$, and (c) $B = 0.50$. Each row represents the times at which the snapshots were obtained 0, 1.0×10^5, 1.0×10^6, and 2.0×10^6 of steps, respectively. Results obtained for a global network of $N = 100$ agents with $T = 0.25$, $E = 0.1$ and $R = 0.25$.

for $B = 0.30$, it happens after 7.0×10^5 steps, but for $B = 0.40$, this occurs after 1.6×10^6 steps, and for greater values, it is not reached in 2.5×10^6 steps.
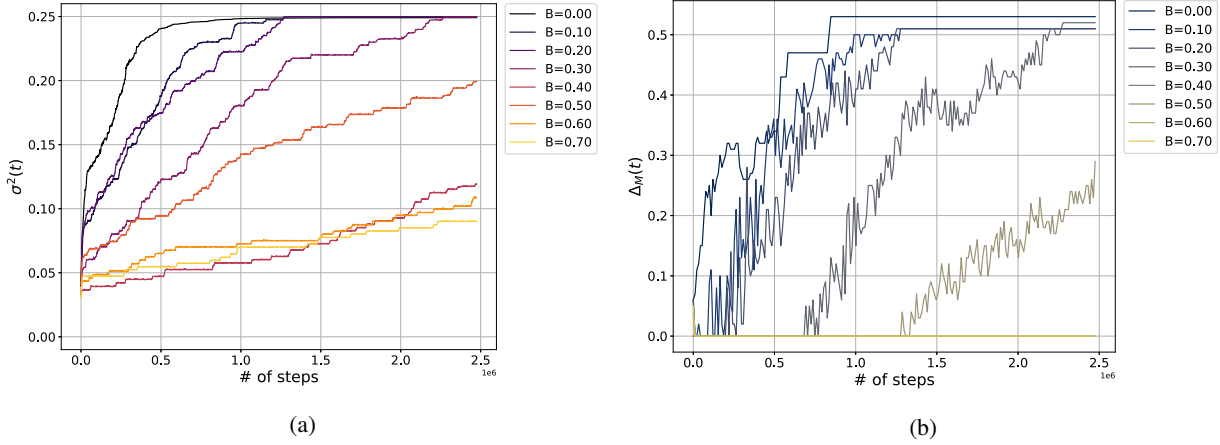
Figure 3.4: Effects of the field intensity B and central message position $x_M = 0.50$ in the system over time. (a) Variance $\sigma^2(t)$ as a function of time. (b) Difference $\Delta_M(t)$ between the largest cluster and the cluster with the same opinion that the media over time. Results for $N = 100$ agents with $T = 0.25$, $E = 0.1$ and $R = 0.25$.

Another interesting observation arises when the media adopts an extremist position. These values are around $x_M = 0.0$ or $x_M = 1.0$. For instance, in Figure 3.5, we observe the progression of agents' opinions when the media adopts an extremist position $x_M = 0.0$. In Figure 3.5 (a), we see the results for $B = 0.10$. For 1.0×10^5 steps, a group is formed in the extreme where the media is located, some actors are in the middle region, and the rest are located around the other extreme. After 1.0×10^6 steps, the system converges to a state with two extreme groups with asymmetrical sizes. Counterintuitively, we find that the largest cluster opinion is located opposite to the opinion of the field. As time passed, the other extreme capitalized more actors that previously were in the middle region. This effect gets more pronounced for high field intensities, as can be observed when comparing Figure 3.5 (a) and Figure 3.5 (b). Indeed, for $B = 0.5$, rapidly (1.0×10^5 steps), most of the population is located near one. Then, the media repels even more this group, and in the end, most of the population is located in the other extreme. The cluster of red nodes expands from around 0.6 of the population for $B = 0.1$ to over 0.8 for $B = 0.5$, exemplifying this heightened shift.

For a more general study, we can analyze the effect of different media positions and field intensities in the system's configuration after 2.0×10^6 steps. In Figure 3.6 (a), we plot the averaged variance over 50 realizations $\langle \sigma^2 \rangle$ against the intensity of the field B for different message positions x_M. As we can see, in general, the media's intervention reduces the system's variance as we increase B. For intermediate values of the media ($x_M = 0.5$), we have that the variance is not reduced for weak-intensity media. However, as we increase the intensity, at around $B = 0.20$, it starts to reduce the system's polarization. In fact, central messages depolarise the most until a variance of $\langle \sigma^2 \rangle = 0.05$ for strong values of B.
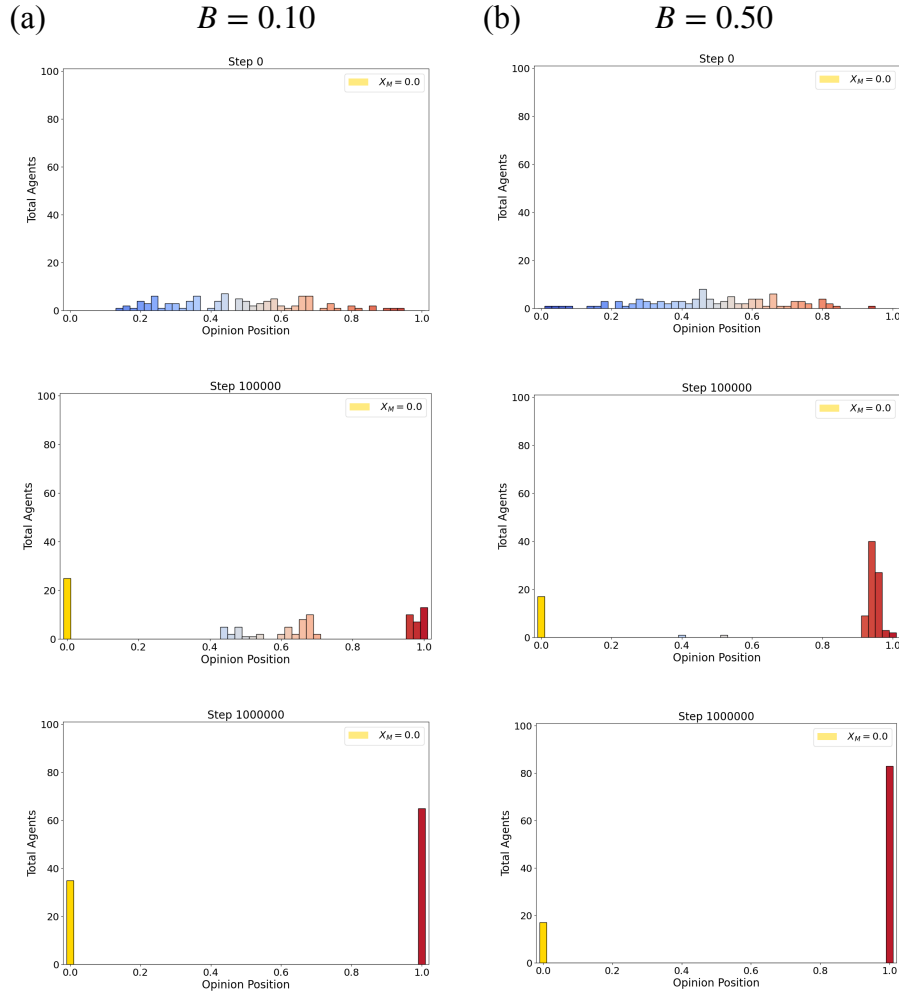
Figure 3.5: Snapshots of the system's time evolution including mass media with an extremist message $x_M = 0.00$. Each column represents a different intensity field B, (a) $B = 0.10$, and (b) $B = 0.50$. Each row represents the times at which the snapshots were obtained 0, 1.0×10^5, and 1.0×10^6 of steps, respectively. Parameters: $T = 0.25$, $E = 0.1$ and $R = 0.25$ for a global network of $N = 100$ agents.

On the other hand, for an extreme position such as $x_M = 1.0$, it reduces more than the central message case for a low-intensity field, and for a high-intensity field, it reduces less than in the central case. This phenomenon is due to the fact that we are reaching a majority in the opposite extreme that is intensified with high values of B.

Finally, for a central right position $x_M = 0.76$, we have a rapid reduction of the polarization for low values of B. The variance is reduced until half of the value of the system without the field for $B = 0.08$. Then, as we increase B,

we get a slight variance increase until around $\langle\sigma^2\rangle = 0.15$. However, after arriving at a threshold B value (around $B = 0.20$), it does not vary anymore, although we increase the intensity of the field.

A more general description of $\langle\sigma^2\rangle$ is shown in Figure 3.6 (b), where we calculate this parameter for a grid of parameters as a function of x_M and B. First, in this graph, we can notice that the results are symmetric with respect to $x_M = 0.50$. Also, we notice that the system has different regions. First, we see that for central message values from $x_M = 0.30$ to $x_M = 0.70$, we get polarized systems for low values of B, but as we increase B, the polarization decreases considerably. This becomes the best policy to consider for the media to reduce polarization in a network. Also, we have the region for central left (or right) messages where we have a rapid decrease in the polarization for low values of B. Then, it stabilizes in an intermediate value of $\langle\sigma^2\rangle$ although we increase B. For the region of extremist messages, we get that for low B values, the system is polarized. However, as we increase it, the system reduces the polarization since we get the asymmetrical extremist groups described in Figure 3.5.

(a)

(b)
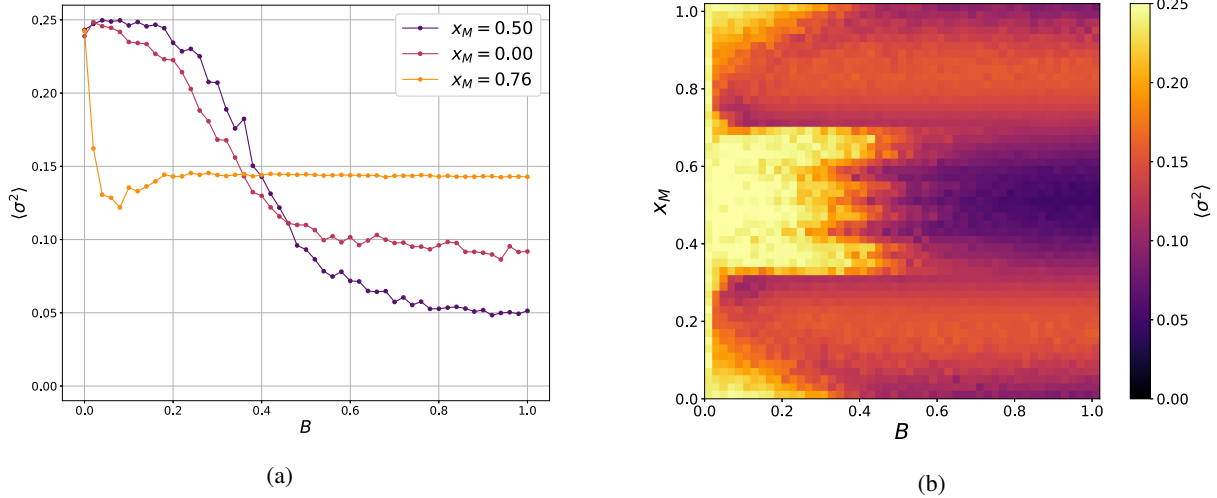
Figure 3.6: Effects of the field intensity B and the message position x_M in the polarization of the opinions after 2.0×10^6 steps. (a) Averaged variance $\langle\sigma^2\rangle$ over 50 iterations as function of B for different values of x_M. (b) A heat map where the color represents the averaged variance $\langle\sigma^2\rangle$ over 20 iterations, and the grid depends on B and x_M. The dark zones mean low polarization, while the yellow zones mean high polarization. Results obtained for a global network of $N = 100$ agents with $T = 0.25$, $E = 0.1$ and $R = 0.25$.

For a better understanding of the size of the largest cluster formed, we analyze the quantities $\langle S_{max}\rangle$ and $\langle\Delta_M\rangle$ as functions of B and x_M. The results are shown in Figure 3.7 (a) and Figure 3.7 (b). We can notice some remarkable results summarized in four regions. First, for weak central messages, we get that the largest cluster is around half of the population, and any of the actors follow the position of the media. Also, considering that the variance is maximum in this region, we are in the region where, after 2.0×10^6 steps, the population becomes extremely polarized.

Second, for a strong central message region with the lowest variance, we get that the largest cluster is over half of the population and follows the mass media message. So, we are in a region where the media attacks a considerable

part of the network. Third, for extreme values of x_M, we notice that the largest cluster is over half of the population, and this size increases with B. However, it does not follow the media message. In fact, we found an asymmetric polarization in this region, with some actors following the media and most of the population on the other extreme position.

Finally, for the central right (or left) media message, we corroborate that the main change of the statistical parameters is for low values of B, and then these stabilize. So, for high intensities, they have no new effects. Here, we see that the size of the largest cluster is slightly larger than half of the population. Also, the difference with the group with the same opinion that the media is small. This means that we have two main clusters, one being the largest and the other a little smaller, which possess the same opinion as the media.

| (a) | (b) |
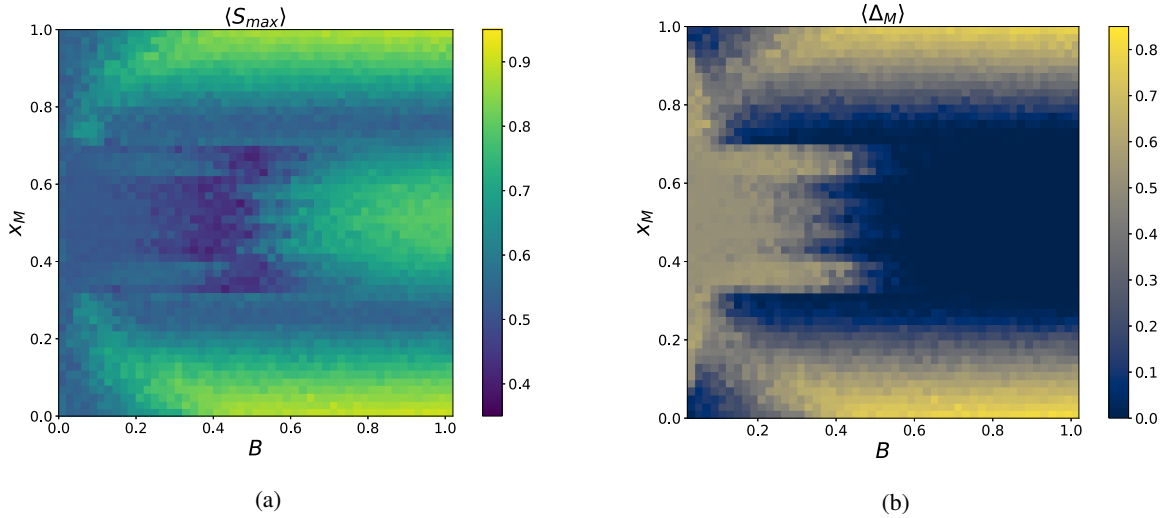
Figure 3.7: (a) Normalized size of the largest cluster $\langle S_{max} \rangle$ as a function of the field intensity B and the message position x_M. (b) Difference Δ_M of sizes between the largest cluster and the cluster with the media opinion on the plane (x_M, B). Results averaging 1000 steps after 2.0×10^6 transients, averaging over 20 realizations for each data point.

3.3.2 Local network

To explore the global field's role on a local network, we consider a ring network where the agents have two neighbors, one on each side, considering boundary conditions. All the agents will be under the influence of an external global field. Figure 3.8 (a) shows the scheme of the resulting network.

The results of the simulations for a system that, without the intervention of the media, would lead to extreme polarization are shown in Figure 3.8. In general, we found that the outcomes of the system are very similar to the ones obtained for the global network. However, there are some differences in the intensity of the statistical quantities calculated. In Figure 3.8 (a), we calculated $\langle \sigma^2 \rangle$ as a function of x_M and B. We can notice that the regions with

extreme polarization for low values of B and central and extremist values of x_M are lower than in the global network case. Also, we see that the results for the central right or left regions are more homogenous across B than in the global network. So, low or high values of B have the same effect on the polarization outcome.

Figure 3.8 (b) shows the normalized size of the largest cluster $\langle S_{max} \rangle$. We see similar results to the fully-connected network. A difference is that we have slightly lower values from central to the central left (or right) x_M values. Another difference is presented in Figure 3.8 (c), where we calculate $\langle \Delta_M \rangle$, we see that for central x_M and low B values, $\langle \Delta_M \rangle$ is lower than in the global case, so there is a greater tendency to follow these kinds of mass media messages. As a result, we can say that the media is more convincing in a local network than in a global one for a central message.

(a)

(b)

(c)

(d)
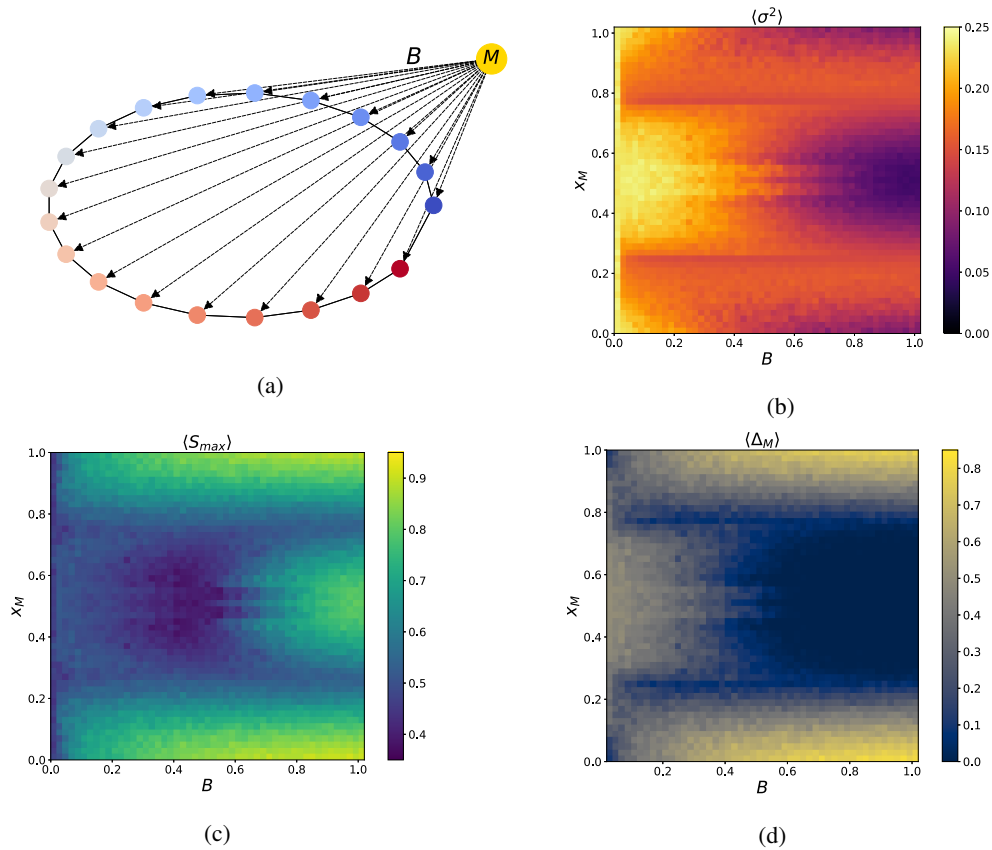
Figure 3.8: (a) Diagram of a ring network including mass media. Statistical quantities as a function of the field intensity B and the message position x_M, (b) variance $\langle \sigma^2 \rangle$, (c) the normalized size of the largest cluster $\langle S_{max} \rangle$, and (d) difference $\langle \Delta_M \rangle$ of the normalized sizes between the largest cluster and the cluster containing the media. Results were obtained for a ring network of $N = 100$ node by averaging 1000 steps after 2.0×10^6 transients and averaging over 20 realizations.

3.3.3 Small world network

Finally, we explore a complex network. Specifically, we reproduce the results for a small world network of $N = 100$ agents with average degree $\langle k \rangle = 4$. Figure 3.9 (a) shows a representation of this network, including the media.

We can see the results in Figure 3.9 for the statistical quantities as a function of B and x_M. In Figure 3.9 (b), we calculated the averaged variance $\langle \sigma^2 \rangle$. Figure 3.9 (c) shows the averaged normalized size of the largest cluster $\langle S_{max} \rangle$ while Figure 3.9 (d) represents the difference $\langle \Delta_M \rangle$ of the largest cluster with the size of the cluster having the media opinion. We notice that the results are similar to those obtained for the global and local networks. In fact, for the mentioned differences between the global and ring networks, we can notice that the small-world network is in the transition between these differences.
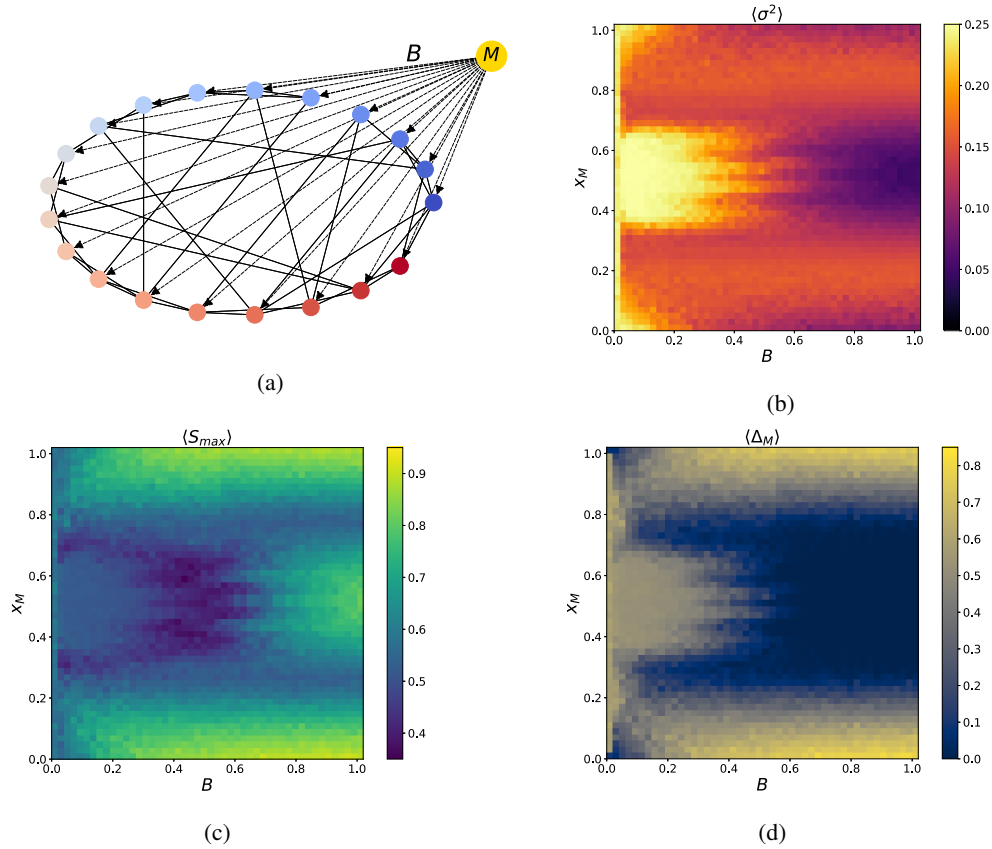
Figure 3.9: (a) Diagram of a small-world network including mass media M with intensity B. Statistical quantities as a function of the field intensity B and the message position x_M, (b) variance $\langle \sigma^2 \rangle$, (c) normalized size of the largest cluster $\langle S_{max} \rangle$, and (d) difference $\langle \Delta_M \rangle$ of the normalized sizes between the largest cluster and the cluster containing the media. Results were obtained for a small-world network of $N = 100$ nodes by averaging 1000 steps after 2.0×10^6 transients and averaging over 20 realizations.

3.4 Results for a highly tolerant population

We can now study the system for a population that, without the media's intervention, would reach a consensus. That is a highly tolerant population. Specifically, we study the system's evolution for $T = 0.40$, $E = 0.1$, and $R = 0.25$ in a global network, including an external global field like the one shown in Figure 3.1.

Figure 3.10 (a) shows the effects on the polarization measure in terms of x_M and B. We notice that in the range from $x_M = 0.4$ to $x_M = 0.6$ (central media opinions), the system still converges to about a single opinion for all values of B. This is corroborated with Figure 3.10 (b) where $\langle S_{max} \rangle$ tends to one for this region. The same result is repeated for low values of B and all the messages' positions of the media. However, as we increase B for central left (or right) to the extremist media messages, we get that the variance of the system starts to grow, increasing the polarization. Also, in Figure 3.10 (b), we notice that from central left (or right) to extremist messages and high values of B, the consensus ($\langle S_{max} \rangle \sim 1$) disappears, and the largest cluster now has a smaller number of agents.
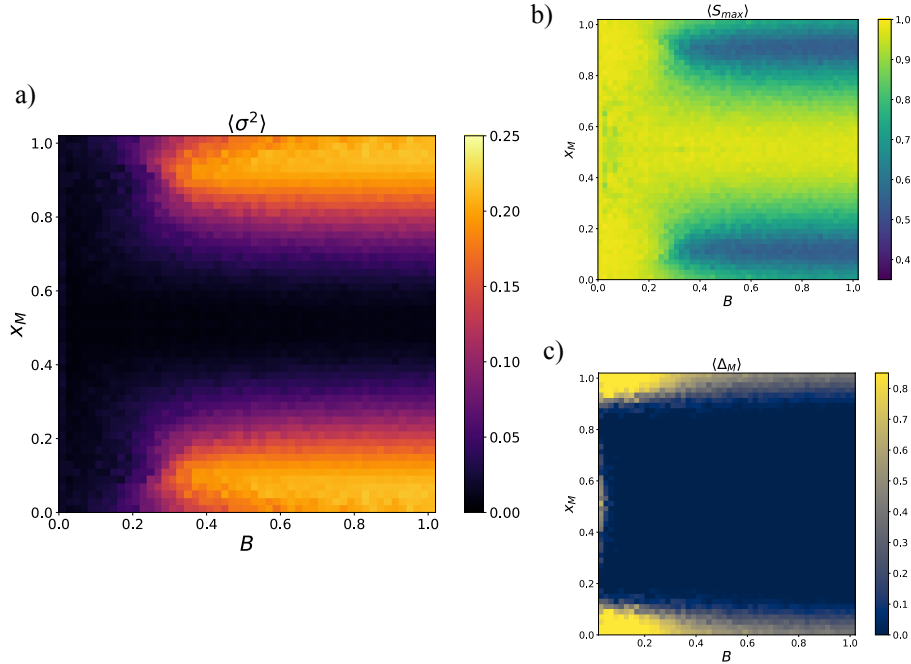
Figure 3.10: Effects of the field intensity B and its message position x_M for each pair (x_M, B) in the (a) variance $\langle \sigma^2 \rangle$, (b) average size of the largest cluster $\langle S_{max} \rangle$, and (c) difference $\langle \Delta_M \rangle$ with the size of the cluster containing the media. Results were obtained for each data point by averaging 1000 steps after 2.0×10^6 transients and averaging over 20 realizations.

Figure 3.10 (c) shows another finding about the opinion that dominates the system. First, without applying the field ($B = 0$), the system reaches consensus in different opinion positions for each simulation. Then, when we include

the field, we notice that it attracts most of the population from $x_M = 0.16$ to $x_M = 0.84$. For this reason, $\langle \Delta_M \rangle$ is zero. For the extreme message values, we have the opposite effect. Although it attracts some actors, the majority group is formed in another cluster, similar to the result of the low-tolerant population.

Chapter 4

The Coevolutionary Attraction-Repulsion Model

In this chapter, we incorporate the rewiring process into the ARM of Axelrold. In Section 2.4, we reviewed the model considering only changes in the opinions of the agents, which means that we had only dynamics for the state variable of the actors. In that model, the links between the nodes were always the same, and the nodes had a certain probability of interacting between them. As discussed in Section 2.6, a system can also have dynamics in the network itself. In this chapter, we create a model with co-evolution where the node dynamics includes the attraction-repulsion rule while the rewiring process is motivated by the Holme-Newman conditions[30] where the disconnections are random, and new links are formed with those with whom the agent is tolerant.

We start the chapter by considering the ARM for a random network, which will be the base topology for applying the rewiring process. Then, we introduce the coevolutive extension of the model. Finally, we analyze the results of the model in terms of the rewiring parameter and the tolerance bound and their impact on the polarization of opinions.

4.1 The Attraction-Repulsion Model in a random network

In the model described in Section 2.4 we explored a global network. Since all the agents were connected between them, it is not possible to apply a rewiring process in this system if we keep constant the number of links in the network. For this reason, we start this chapter by exploring the ARM in another network where each node i has a different set of neighbors v_i that allows us to break edges and then create new connections.

First, we simulate the different scenarios without changes in the topology in a random network with an average degree $\langle k \rangle = 4$. This means that all the nodes have, on average, four neighbors, creating a local network. A particular case is shown in Figure 4.1 where we simulate the system for the parameters $T = 0.20$, $E = 0.1$ and $R = 0.25$ for a random network of $N = 100$ actors. As observed, this system evolves from an initial Gaussian distribution in the

actors' opinions (Figure 4.1 (a)) to a state of maximum polarization (Figure 4.1 (b)) after approximately 5.0×10^5 steps. In the final network, coexistence between extreme positions is evident, with half of the population adopting an extremist left position and the other half holding an extremist right position. Nevertheless, there are many links joining agents with these contrary opinions.

(a)   (b)
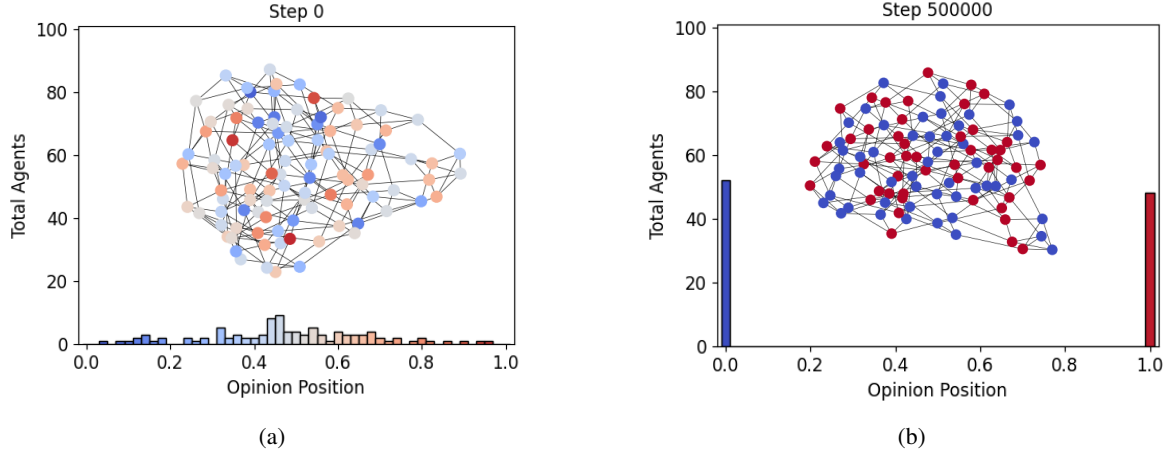
Figure 4.1: Initial and final states of a system of the Attraction-Repulsion Model in a random network of 100 agents with $\langle k \rangle = 4$ considering $R = 0.25$, $T = 0.20$, and $E = 0.1$. The system underlies an evolution of the distribution of opinions from (a) a Gaussian distribution at the beginning to (b) an extremely polarized at the convergent state.

The general results for these systems are shown in Figure 4.2. Similar to previous chapters, we quantify the polarization by the averaged variance over realizations $\langle \sigma^2 \rangle$ for the asymptotic state. $\langle \sigma^2 \rangle = 0$ means convergence to a single opinion while $\langle \sigma^2 \rangle = 0.25$ implies an extreme polarization. Figure 4.2 (a) shows the variance after 1.0×10^6 steps in terms of the responsiveness R and tolerance T, keeping fixed the exposure E. Figure 4.2 (b) shows the variance after 2.0×10^6 steps in terms of E and T, keeping fixed R. We can notice that both phase diagrams (R, T) and (E, T) are almost equal to the ones calculated for the global network in Section 2.4 in Figure 2.6 (b) and Figure 2.7 (b), respectively. This implies an interesting result: the polarization outcomes in the ARM are independent of whether the network is local or global.

A motivating result for considering rewiring based on homophily is shown in Figure 4.2 (b). Here, the polarization in the region for low tolerance $T \leq 0.30$ has an interesting dependence on the exposure E. As we see, in the region of low values of E, we get less polarization than for high values of E, where we reach extreme polarization. Thus, adding rewiring could be an effective mechanism that can reduce polarization by limiting repulsive interaction among intolerant actors with different opinions.

(a)   (b)
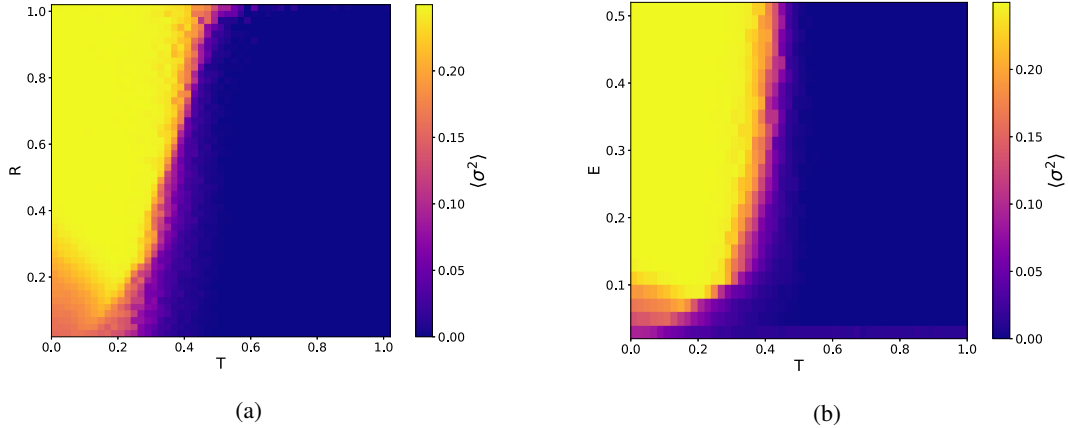
Figure 4.2: Phase diagrams representing the averaged variance over 20 realizations for a random network of $N = 100$ agents with $\langle k \rangle = 4$ for (a) (R, T) and (b) (E, T) grids after 1.0×10^6 steps and 2.0×10^6 steps respectively. Yellow means extreme polarization, while dark blue means convergence to a single opinion.

4.2 The Coevolutionary Attraction-Repulsion Model

We consider an Erdős–Rényi or random network of N nodes $\{i = 1, \cdots, N\}$ with mean degree $\langle k \rangle = 4$ that represents social agents. Each node i has a set of neighbors $v_i(t)$ of degree k_i which may vary in time. Also, each agent has a state variable $x_i(t) \in [0, 1]$ that represents an opinion. In the beginning, all the opinions are initiated following a Gaussian distribution with a mean of 0.5 and a standard deviation of 0.2 (see Section 2.4 for an explanation of these conditions). Then, at each step time, an agent, i, can have both changes in its set of neighbors or in its state. So, we introduce the probability of rewiring P_r to control how many interactions occur in the topology. With a probability P_r, we apply the link update process, and with probability $(1 - P_r)$, the interactions are in the nodes' opinions. In the limit $P_r \to 1$, we have only updates in the network links. On the other hand, in the limit $P_r \to 0$, we have only changes in the opinions. This limit case corresponds to the system studied in Section 4.1 given by only the ARM.

For the topology dynamics of an agent i, we randomly select an agent j from its neighbors and cut their link. Subsequently, we choose an agent l such that $|x_i - x_l| < T$, and we create a link between them. Each disconnection process is followed by creating a new link, so we keep both the total number of links and the average degree of the network $\langle k \rangle$ constant. This rewiring process is based on the homophily principle, where agents only connect with the actors whose opinion is inside their confidence threshold. In the space of parameters (d, r) discussed in Section 2.6, these criteria of disconnection and connection correspond to the values $(d, r) = (0.5, 1)$, commonly referred to as the Holme-Newman conditions [30].

An illustration of the rewiring mechanism is provided in the upper part of Figure 4.3. In the figure, the color of the nodes represents their opinions, ranging from the bluest nodes representing an opinion $x = 0$ to the reddest representing an opinion $x = 1$. As we see, with probability P_r, the agent i (sky blue) disconnects from a randomly selected neighbor j and then connects with a similar node l (blue).

On the other hand, for the opinions dynamics, we consider the two rules of the ARM mentioned in Section 2.4. The first is that the probability of interaction between two agents i and j is given by $(1/2)^{d_{ij}/E}$ where d_{ij} is their opinion distance. The second is the attraction-repulsion rule, where interactions are attractive if d_{ij} is inside the tolerance threshold ($d_{ij} \leq T$) and repulsive if it is outside ($d_{ij} > T$). For simplicity, we use the same parameter of tolerance T for both the node and the rewiring dynamics. So, agents will use the same confidence-bounded threshold for having attractive interactions and creating new connections.

An illustration of the nodes' dynamics is presented in the lower section of Figure 4.3. As we see, with probability $1 - P_r$, we calculate the probability of interaction between agent i and a randomly selected neighbor j. Then, we apply the attraction-repulsion rule where we notice that agent i approaches agent j if their opinion distance is inside the threshold; otherwise, it moves away.
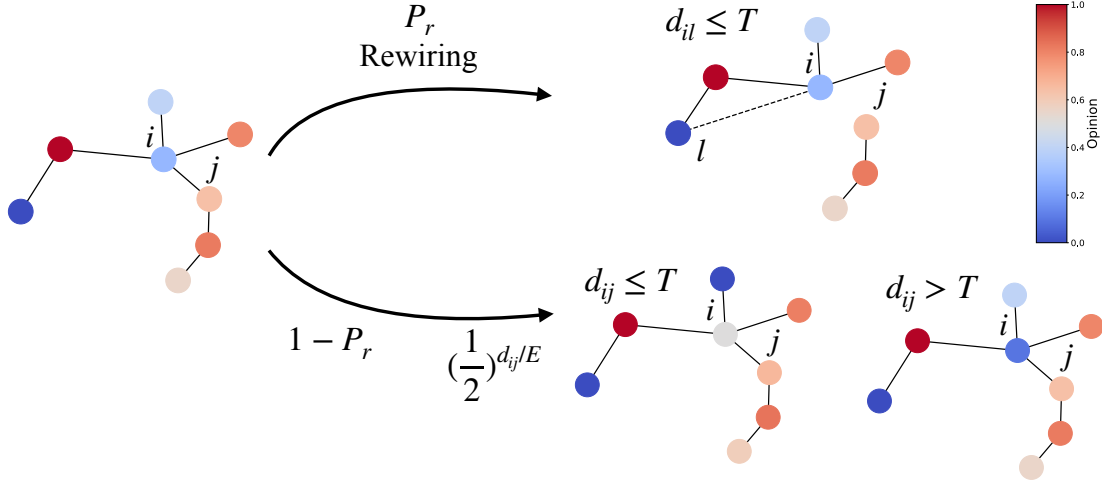
Figure 4.3: Schematic illustration of the coevolutive model. With probability P_r, the rewiring process takes place where the agent i breaks random a link with one of its neighbors and creates a new link with an agent l that has a similar opinion inside its confidence bound T. On the other hand, with probability $1 - P_r$ we apply the attraction-repulsion rule.

The dynamics of the system follows this iterative algorithm:

1. Randomly chose an active agent i.

2. With probability P_r apply the rewiring process. Select randomly an agent $j \in v_i$ such that $k_j \geq 2^*$. Then, (i) break the link between agents i and $j^\dagger$. (ii) Select random an agent $l \notin v_i$ such that $|x_i - x_l| < T$ and create the link between nodes i and l.

---

*We apply this condition to prevent isolated nodes.

$\dagger$In this step, we have to ensure that there exists a node $l \notin v_i$ such that $|x_i - x_k| < T$, to create a new link and complete the rewiring process. Otherwise, we proceed to select another agent i.

3. With probability $1 - P_r$ apply the node dynamics. (*i*) select the source of attention *j*. (*ii*) Calculate the probability of interaction between agents *i* and *j* given by $(1/2)^{d_{ij}/E}$ where $d_{ij} = |x_i - x_j|$. (*iii*) For a successful interaction, if $d_{ij} \leq T$, agent *i* approach agent *j* an amount of *R* times d_{ij}. Otherwise agent *i* moves away from agent *j*, a number of *R* times d_{ij}

A flowchart that illustrates this algorithm is shown in Figure 4.4.
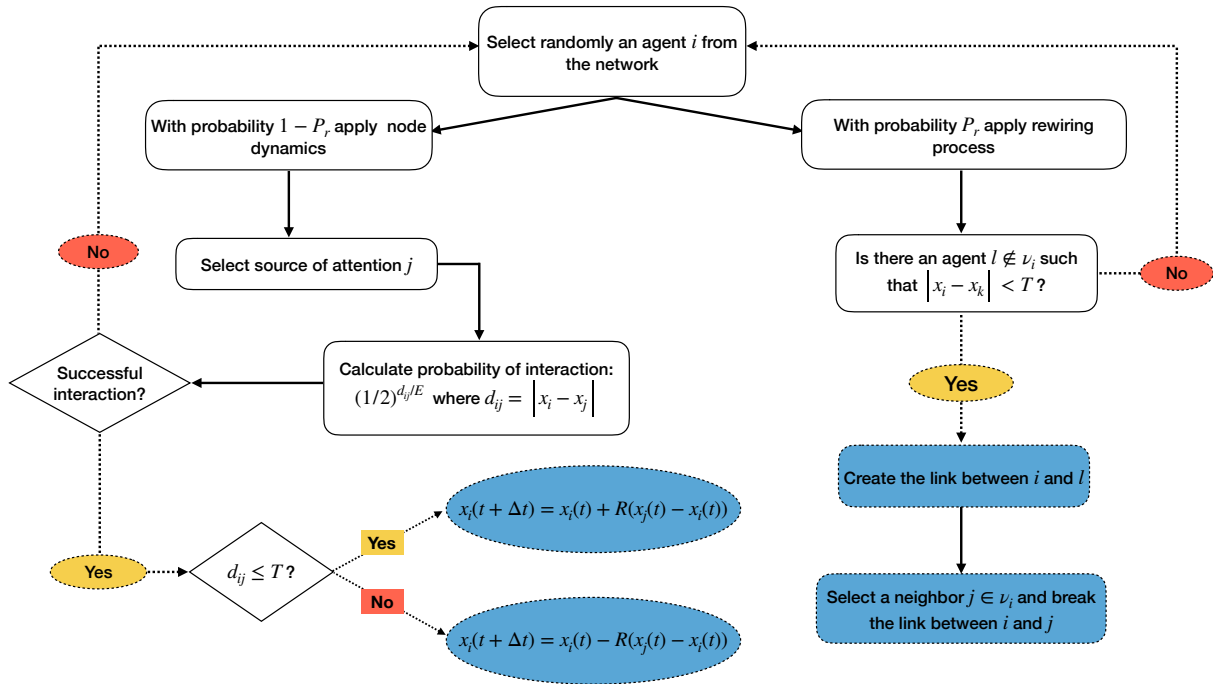
Figure 4.4: Flowchart of the algorithm for the Coevolutionary Attraction-Repulsion Model.

Our source code for this model can be found in Appendix B. To optimize the code, we implement a stop condition where if the variance of the system does not change within a range of 10^{-6} over 5×10^4 steps, the program stops. Therefore, the computational cost depends on whether the system reaches a converged state or not[*]. The time expenses also vary depending on whether it is interested in studying the entire simulation history or just the asymptotic state[†]. The source code includes a function to measure the time of each simulation.

All the parameters that intervene in the model dynamics are summarized in Table 4.1. In our pursuit of preventing

---

[*]For example, using the parameters $T = 0.20$, $E = 0.1$, and $R = 0.25$, a system with $P_r = 5 \times 10^{-3}$ takes around 30 seconds to complete a simulation, while a system with $P_r = 5 \times 10^{-4}$, takes around 3 minutes. Due to the stochasticity of the model, each repetition of a simulation has a slightly different convergence time.

[†]For reference, in the mentioned system with $P_r = 5 \times 10^{-3}$, the simulation time can increase from 30 seconds to around a minute and a half if we save the entire history. Similarly, for the scenario with $P_r = 5 \times 10^{-4}$, the simulation time extends from approximately 3 minutes to around 9 minutes when the entire history is saved.

polarization, we configure the parameters to ensure that without rewiring, the system would tend toward a polarized state. We will then study the evolution of the system for different values of probability of rewiring P_r and tolerance T, which are the parameters that mainly intervene in the topology dynamics.

Parameter	Symbol	Meaning	Default Value
Rewiring Probability	P_r	Probability of having dynamics on the topology	$[0-1]$
Tolerance	T	Distance threshold within which two agents can get connected. Also, distance within interactions are attractive and beyond are repulsive	$[0.1-0.25]$
Responsiveness	R	The fractional distance an actor's ideological position moves as a result of an interaction	0.25
Exposure	E	The degree to which actors interact with dissimilar points of view expressed as the halving distance	0.1 & 0.5
Number of Agents	N	Actor that belong to the network	100
Initial Mean and Standard Deviation	μ_0, σ_0	Characterized the initial distribution of the agents opinion's	$0.5, 0.2$

Table 4.1: Parameters used in the Coevolutionary ARM.

4.3   Results

We initiate our analysis with a system that would naturally evolve into maximum polarization if rewiring links were not introduced ($T = 0.2$, $R = 0.25$, $E = 0.1$). Figure 4.5 shows snapshots of the network for different values of P_r for each column and different time steps for each row.

For a low rewiring probability $P_r = 5.0 \times 10^{-4}$, shown in Figure 4.5 (a), the system exhibits the following behavior. Initially, after 1.0×10^5 steps, polarized opinions coexist in the same network. Subsequently, after 1.0×10^6 steps, two distinct clusters with opposing viewpoints emerge, displaying strong internal connectivity but limited inter-cluster links. Such clusters, characterized by sharing and disseminating the same content, are often called "echo chambers"[54]. Echo chambers have been experimentally observed in social networks[11, 12], and there is currently significant interest in developing theoretical models to understand them[55, 56]. In this regard, an extension of our model can provide a theoretical framework for studying the formation of echo chambers. Finally, at 2.0×10^6 steps, the system has already converged into a fragmented network, with approximately half of the population embracing one extremist viewpoint and the other half adopting the totally opposite opinion.

However, a central group starts to emerge as we increase the rewiring probability, e.g., for $P_r = 5.0 \times 10^{-3}$. In Figure 4.5 (b), we see that after 5.0×10^4 steps, the system coexists with two extremist groups and a cluster of actors with central opinions. At 1.5×10^5 steps, the system forms three distinct communities, with two of them leaning
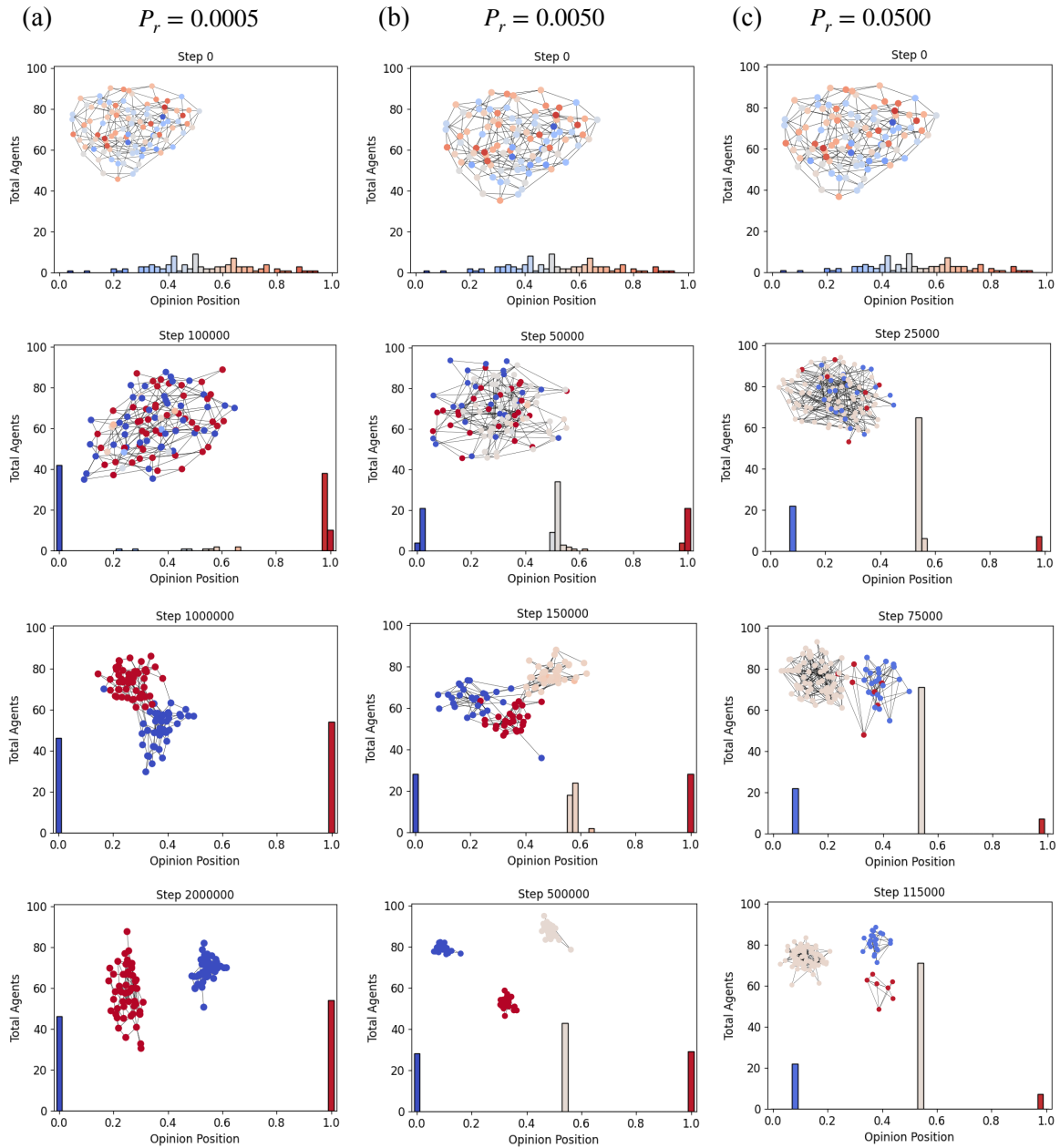
Figure 4.5: Snapshots of the system's time evolution for different rewiring probabilities. Each column represents a different P_r, and each row represents the times at which the snapshots were obtained. (a) For $P_r = 5.0 \times 10^{-4}$, (b) $P_r = 5.0 \times 10^{-3}$, and (c) $P_r = 5.0 \times 10^{-2}$. Parameters: $T = 0.20$, $E = 0.1$ and $R = 0.25$ for an initial random network with $\langle k \rangle = 4$ of $N = 100$ agents.

toward extremist opinions and the third cluster maintaining central viewpoints. These communities have limited interconnections. Finally, after 5.0×10^5 steps, the communities break their links, and the system converges in a state with three network fragments, where two of them have opinions at each extreme, and the largest one has a central opinion.

This effect intensifies by increasing P_r. Figure 4.5 (c) displays snapshots of the system's evolution for $P_r = 5.0 \times 10^{-2}$. After 2.5×10^4 steps, a predominant central group coexists with actors close to $x = 0$ and $x = 1$ opinions. Then, at 7.5×10^4 steps, these groups give rise to the presence of three communities. Finally, at 1.15×10^5 steps, the communities fragment into three components. We see that the cluster possessing a central opinion becomes the majority of the population. Notice that this emergent central group has substantially increased its size from around 40% of the population in the $P_r = 5.0 \times 10^{-3}$ case to about 70% of the actors for $P_r = 5.0 \times 10^{-2}$.

Comparing the three scenarios, we notice that there is a faster convergence to the final state as we increase P_r. Also, interestingly, we observe that the emergent central group varies its location near the opinion position $x = 0.5$ in each repetition of the simulation. For example, if we repeat the simulation 50 times with $P_r = 5.0 \times 10^{-2}$, the central group, on average, is located at $\overline{x} = 0.494 \pm 0.102$, where the error 0.102 represents the standard deviation across realizations. When $P_r = 5.0 \times 10^{-3}$, the central group is located at $\overline{x} = 0.493 \pm 0.083$ on average.

To gain deeper insights into how the emergent central group contributes to the reduction in system polarization over time, we examine the evolution of variance $\sigma^2(t)$ over time for different P_r values in Figure 4.6. In Figure 4.6 (a), which corresponds to $T = 0.20$, we observe several trends. Initially, without rewiring ($P_r = 0$), the system reaches maximum polarization after 1.0×10^6 steps. For low P_r values ($\leq 1.0 \times 10^{-3}$), the system exhibits near-maximum polarization and converges at approximately 4.0×10^5 steps. Here, we do not have the presence of the central group, and the system only fragments into two clusters. However, as we increase the rewiring to $P_r \geq 5.0 \times 10^{-3}$, the reduction in polarization becomes apparent, with this effect becoming more pronounced with higher P_r values. Notably, for $P_r \geq 5.0 \times 10^{-2}$, the variance decreases to $\sigma^2 \leq 0.10$. Additionally, we observe that increasing P_r leads to quicker convergence to a stable state.

We have also studied the case for $T = 0.25$ in Figure 4.6 (b). We see that the network for $P_r = 0.0$ converges to a state of maximum polarization after 1.5×10^6 steps. As expected, when we apply the rewiring, the polarization levels decrease more significantly than in the case of $T = 0.20$. We see that for values $P_r \geq 5.0 \times 10^{-3}$, we get values $\sigma^2 \leq 0.10$, and these continue decreasing with P_r. This region corresponds to the emergence of the central cluster with high levels of population.

We proceed to quantify the size of the emergent central group. Similar to Section 3.2, we define a cluster s_ξ as the set of elements belonging to the same interval I_ξ of size $\epsilon = 1/K$, where K represents the total number of clusters within the range $[0, 1]$. In this context, a cluster ξ has a central opinion if its interval lies in the central region. We consider that an interval is located in a central region when $I_\xi \in [0.24, 0.76]$. We then define $S_{central}(t)$ as the normalized size of the largest cluster with a central opinion at time t. $S_{central}(t_f)$ represents this largest cluster at the asymptotic state. Additionally, we define $\langle S_{central} \rangle$ as the average normalized size of the largest central cluster size over n realizations at the asymptotic state, given by:

$$\langle S_{central} \rangle = \frac{1}{n} \sum_{i=1}^{n} S^i_{central}(t_f). \tag{4.1}$$

(a)   (b)
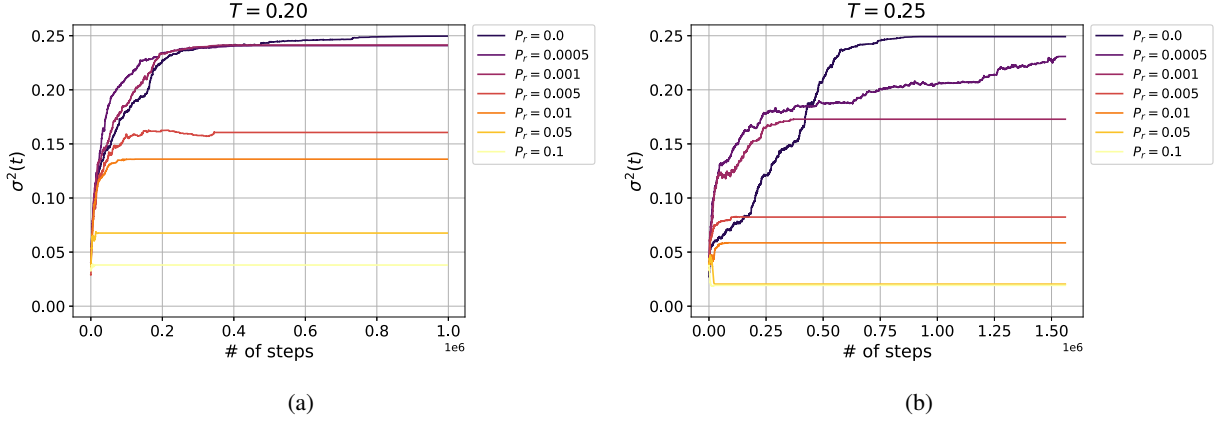
Figure 4.6: Variance $\sigma^2(t)$ as a function of time for different values of rewiring P_r, for (a) $T = 0.20$ and (b) $T = 0.25$. Default parameters are $E = 0.1$ and $R = 0.25$ for a random network of $N = 100$ agents with $\langle k \rangle = 4$.

In Figure 4.7 (a), we observe the behavior of $\langle S_{central} \rangle$ at the asymptotic state in relation to the probability of rewiring P_r. We notice that for different values of tolerance, there is a critical P_r^* value where the central group emerges. This suggests a phase transition, where there is a critical value P_r^* for each T value. Lower tolerance populations require a higher P_r^* value for this transition. Furthermore, after the emergence of this cluster, its size increases with P_r. In fact, the size of this group can overcome half of the population for sufficiently high rewiring values. For a highly tolerant population, this group could become the whole population. As previously mentioned, the central group's location can fluctuate around the center, leading to differing consensus opinions across simulations. These fluctuations arise from the probabilistic dynamics of the model and the variability in initial conditions. On average, the central group is situated at $\overline{x} = 0.5$ with a standard deviation of approximately ± 0.1.

The emergence of this central group directly impacts the system's polarization. Figure 4.7 (b) shows the averaged variance over realizations $\langle \sigma^2 \rangle$ as a function of P_r for different tolerance values. The effect of reducing polarization by introducing rewiring becomes evident, particularly as P_r increases. This effect leads to a decreasing curve, transitioning from extreme polarization to low values $\langle \sigma^2 \rangle \leq 0.05$. This effect is also achieved for low values of tolerance. The logarithmic scale we are using for P_r is due to the high sensitivity that the variance has for low values of P_r.

In Figure 4.7 (c) and Figure 4.7 (d), we repeat these calculations with a higher exposure value, $E = 0.50$. The increased exposure implies a higher likelihood of agent-agent interaction, increasing the rate of opinion dynamics. In Section. 2.4 we see how this probability of interaction behaves in Figure 2.3 (c).

As we see in Figure 4.7 (c), with the exposure value $E = 0.50$, the transition for having a central cluster occurs in the P_r range of 10^{-1}, in contrast to the $E = 0.1$ case where transitions occur within the range of 10^{-4} to 10^{-2}. In Figure 4.7 (d), we see that also the variance starts to reduce significantly in the range of 10^{-1}. Although we need a higher P_r value, we can decrease the polarization of the network significantly.

This reflects the competition between the dynamics of the nodes and the topology. While the first converges
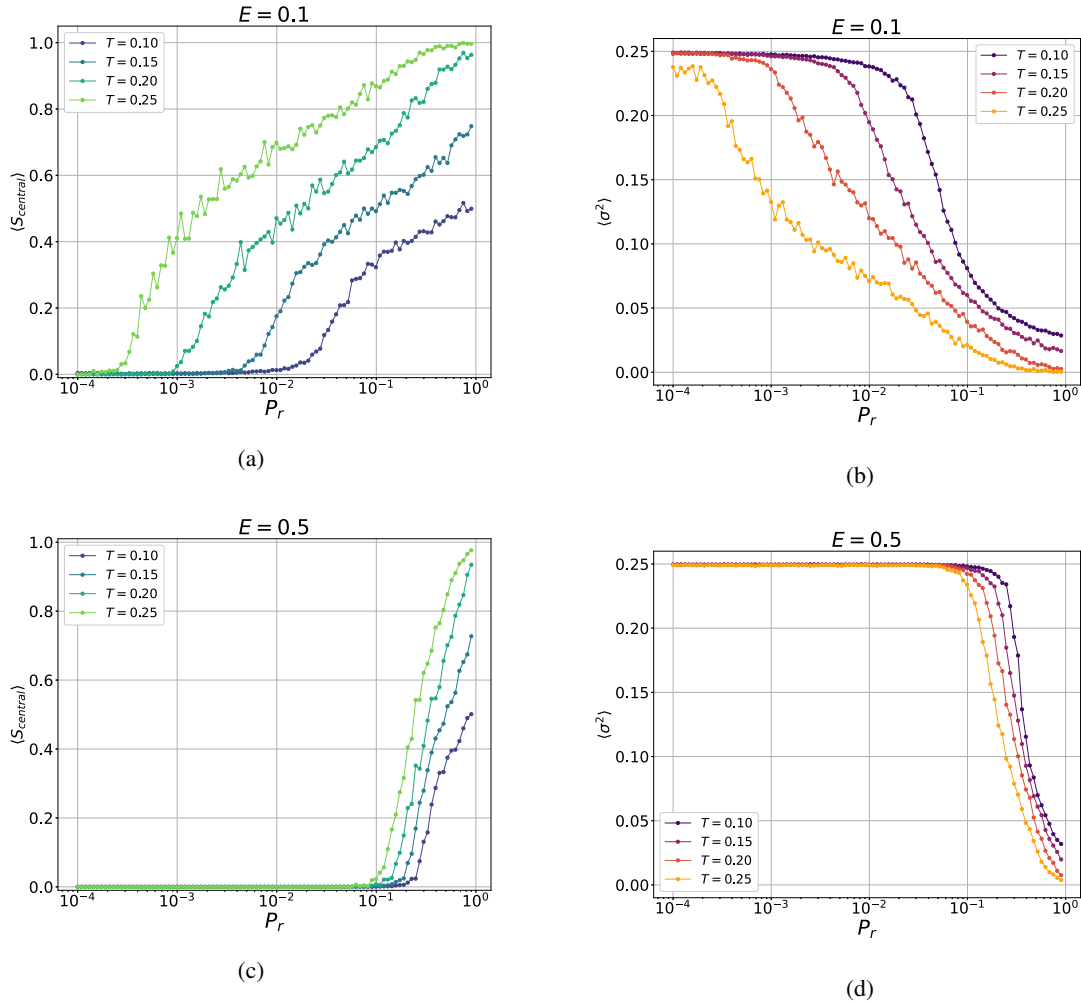
Figure 4.7: Averaged normalized size of the largest cluster belonging to a central group over realizations $\langle S_{max} \rangle$ as a function of P_r for (a) $E = 0.1$ and (c) $E = 0.5$. Averaged variance over realizations $\langle \sigma^2 \rangle$ as a function of P_r for (b) $E = 0.1$ and (d) $E = 0.5$. Results calculated for $N = 100$ averaged over 50 realizations on a random network with $\langle k \rangle = 4$ for constant $R = 0.25$.

to maximum polarization, the second converges to agreement. Thus, these findings align with the hypothesis that minimizing interactions between dissimilar agents is an effective way to prevent or control polarization. In summary, our model predicts that a high degree of rewiring based on homophily can prevent a system that would otherwise undergo extreme polarization.

Chapter 5

Conclusions & Outlook

In this work, we have been able to implement and reproduce the results of the recent Attraction-Repulsion Model (ARM) for the polarization of opinions proposed by Axelrod. *et al.* This agent-based model considers that actors with similar opinions are more likely to interact, and those interactions are attractive, while dissimilar agents have less probability of interacting, and those interactions are repulsive. Low tolerance leads to extreme polarization, while high tolerance converges to consensus. Responsiveness (R) mainly influences the speed of reaching a convergence state. Exposure (E) affects polarization, with low values preventing it and high values exacerbating it, particularly among intolerant agents. After analyzing that model, we have extended it in two ways: *i*) adding a global field and *ii*) making it coevolutive in opinions and connections.

First, we include the mass media as an external global field characterized by its intensity B and message position x_M. The model incorporates the feature that media is more likely to interact with agents with similar opinions than those with different views. Also, the model allows the mass media to have attractive or repulsive effects on the agents, depending on their bounded confidence.

We found that a central mass media message can slow down the process of polarization for a system that, without the action of the field, would evolve to maximum polarization. This is achieved by attracting actors to take an opinion similar to the media. On the other hand, when the media takes an extremist message, it repels actors to the other extreme, generating an asymmetric polarization with most of the population located in the opposite position of the media message. Local networks exhibited similar trends, but the media's persuasiveness was higher for central messages. Complex networks, such as small worlds, fall between global and local networks in terms of polarization behavior.

For a highly tolerant population that reaches agreement without the field's intervention, we found that when the media had central opinions (between $x_M = 0.4$ and $x_M = 0.6$), the system consistently achieved consensus, irrespective of the field's strength (B). In this region, we observed that the field attracted the population to its opinions for central media messages, resulting in no difference ($\langle \Delta_M \rangle = 0$) between the cluster having the media opinion and the largest cluster. However, for extremists and central left or right messages, increasing the field intensity leads to higher variance and a more polarized population composition. In this case, the majority forms a

43

distinct cluster from the media messages, similar to low-tolerant populations.

We have also introduced a Coevolutionary Attraction-Repulsion Model as a general framework for investigating the interplay between opinion dynamics and topology evolution. We have presented a detailed algorithm for the coevolutionary model, combining opinion dynamics based on attraction and repulsion with a rewiring process to connect agents with similar opinions. We have examined the impact of varying the rewiring probability (P_r) on the system behavior through several simulations. We have observed that by varying the probability of network rewiring (P_r), we could effectively control the polarization dynamics in the system. Specifically, as P_r increases, a central group of moderate opinions emerges, significantly reducing overall polarization. This phenomenon is accompanied by a faster convergence to stable states, highlighting the importance of network rewiring in mitigating polarization. Furthermore, our results revealed the occurrence of phase transitions depending on P_r and tolerance levels, shedding light on the critical parameters that influence polarization dynamics. Overall, the coevolutive model offers valuable insights into strategies for managing polarization in complex social networks, emphasizing the role of network dynamics in shaping collective opinions.

In summary, the main contribution of the present thesis is that we have found two mechanisms that can control or eliminate polarization of opinions: *i*) Global mass media with moderate messages in the opinion spectrum, *ii*) Rewiring the social network based on homophily.

For future work, it would be valuable to extend the study to investigate the dynamics of polarization in heterogeneous populations, where individuals possess varying levels of tolerance. Exploring how polarization patterns emerge in networks with diverse tolerance parameters could provide insights into real-world scenarios where individuals exhibit varying degrees of open-mindedness.

Another interesting feature for exploring is to incorporate alternative criteria for network rewiring. By introducing lower levels of homophily during the establishment of new connections, we can avoid network fragmentation. This approach may yield diverse outcomes within the system. For example, it could result in the coexistence of a minority of extremists alongside a predominant central group for high values of rewiring. Conversely, when rewiring occurs less frequently, it may preserve the formation of echo chambers over time. Consequently, the Coevolutionary Attraction-Repulsion Model can serve as a valuable theoretical mechanism for the formation of echo chambers, a topic highly discussed nowadays.

Appendix A

Computer Code for the Attraction-Repulsion Model with a Mass Media

In this appendix, we provide our own code for simulating the Attraction-Repulsion Model, including mass media as an external global field. This code was developed in Python by using the library NetworkX. The program can generate data for only the asymptotic data or save the complete simulation history. Consequently, the code's outputs can be a text file containing nodes' opinions for the last one thousand steps or a text file that records the history of nodes' opinions for every N steps. To obtain estimates of computational time, you can enable time measurement by modifying the `trange` function as follows: `disable=False`.

The program includes functions for creating global, ring, and small-world networks with mass media. All our statistical calculations were conducted using these output files. In the final section, the script incorporates the experiment `expA_grid` that generates the data for the asymptotic states data for a grid 50×50 for B and x_M over twenty iterations. The code is parallelized using the `multiprocessing` library.

A more comprehensive version of the code that also adds the statistical analysis with the respective instructions can be found in the GitHub repository **https://github.com/mateocarpio/ARM-Global-Field**.

```python
#!/usr/bin/env python

#import libraries
import networkx as nx
import numpy as np
from tqdm import trange
```

```python
import math
from itertools import product
import os
import multiprocessing as mp

#Class to run and save the simulatios
class ARM_MM():
    def __init__(self, params, iters, seed, savehist=True):
        defaults = {'B' : [0.25], 'XM' : [0.0], 'N' : [101], 'E' : [0.1], 'T' :
            [0.25], 'R' : [0.25], 'S' : [500000]}
        plist = [params[p] if p in params else defaults[p] for p in defaults]
        self.params = list(product(*plist))
        self.iters = iters
        self.rng = np.random.default_rng(seed)
        self.savehist = savehist

    #Create intial opinions with the Mass Media opinion as the last node
    def initializing(self, N, XM):
        config = np.zeros(N)
        config[N-1] = XM
        for i in np.arange(N-1):
        #initial Gaussian distribution
            while True:
                config[i] = self.rng.normal(0.5, 0.2)
                if 0 <= config[i] and config[i] <= 1:
                    break
        config = config.reshape(-1, 1)
        init_config = config
        return config

    #Create complete network with MM
    def complete_graph_MM(self, N, config):
        G=nx.complete_graph(N)
        for i in G.nodes:
            G.add_nodes_from([i], opinion=config[i])
        return G

    #Create ring network with MM
    def circulantMM(self, N, config):
        G=nx.circulant_graph(N, [1])
        for i in G.nodes:
```

```python
47              G.add_nodes_from([i], opinion=config[i])
48          #Including Mass Media
49          G.add_nodes_from([N-1], opinion=config[N-1])
50          #Add connections between the MM and all the nodes
51          for i in G.nodes:
52              if i!=N-1:
53                  G.add_edge(N-1, i)
54          return G

56      #Small-world network including Mass Media
57      def small_world_MM(self, N, config):
58          G=nx.watts_strogatz_graph(N - 1, 4, 0.3)
59          contador=0
60          for i in G.nodes:
61              G.nodes[i]['opinion'] = config[i]
62              contador=contador+1
63          #Including Mass Media
64          G.add_nodes_from([N-1], opinion=config[N-1])
65          for i in G.nodes:
66              if i!=N-1:
67                  G.add_edge(N-1, i)
68          return G

70      #Save the data in a .txt file
71      def save_data(self, G, iters, step, directory_name):
72          if step == 0:
73              with
                      open(f"./outputfolder/{directory_name}/history_iteration-{iters}.txt",
                      "w") as f:
74                  for k in G.nodes:
75                      f.write(str(k) + "\t")
76                  f.write("\n")
77          with open(f"./outputfolder/{directory_name}/history_iteration-{iters}.txt",
                "a") as f:
78              for k in G.nodes:
79                  f.write("{:.6f}\t".format(G.nodes[k]["opinion"][0]))
80              f.write("\n")

82      #Save the last 1000 steps
83      def asymptotic_data(self, G, iters, step, S, directory_name):
84          if step == S-1000:
```

```python
            with
                open(f"./outputfolder/{directory_name}/asymp_steps_iter-{iters}.txt",
                "w") as f:
                for k in G.nodes:
                    f.write(str(k) + "\t")
                f.write("\n")
        with open(f"./outputfolder/{directory_name}/asymp_steps_iter-{iters}.txt",
            "a") as f:
            for k in G.nodes:
                f.write("{:.6f}\t".format(G.nodes[k]["opinion"][0]))
            f.write("\n")

    #Dynamics of the network
    def arm_MM(self):
        for param in self.params:
            B, XM, N, E, T, R, S = param
            directory_name = "B_{:.2f}-XM_{:.2f}".format(round(B, 2), round(XM, 2))
            if not os.path.exists("./outputfolder/"+str(directory_name)):
                os.makedirs("./outputfolder/" + str(directory_name))
            for it in range(self.iters):
                config = self.initializing(N, XM)
                G = self.circulantMM(N,config)
                for step in trange(S, desc='Simulating interactions', disable=True):
                    #Choose a random node except mass media
                    i = self.rng.choice(np.delete(G.nodes,-1))
                    #Choose j as Mass Media with probability B
                    if self.rng.random() <= B:
                        j = N-1
                    else:
                        #Choose a random neighbor with probability 1 - B
                        j = self.rng.choice(np.delete(G[i],len(G[i])-1))
                    #Calcualte distance between opinions
                    dist = (abs(G.nodes[i]["opinion"] - G.nodes[j]["opinion"]))
                    #Calculate probability of interaction
                    prob = math.pow(0.5, dist/E)
                    if self.rng.random() <= prob:
                        #Condition for atrarction d < T
                        if dist <= T:
                            #i get closer to j, R times their distance
                            G.nodes[i]["opinion"] = G.nodes[i]["opinion"] + R *
                                (G.nodes[j]["opinion"] - G.nodes[i]["opinion"])
```

```python
122                        else:
123                            #Condition for repulsion d > T
124                            G.nodes[i]["opinion"] = G.nodes[i]["opinion"] - R *
                                  (G.nodes[j]["opinion"] - G.nodes[i]["opinion"])
125                        #Set limits [0-1]
126                        G.nodes[i]["opinion"] = np.maximum(0,
                              np.minimum(1,G.nodes[i]["opinion"]))
127                    #Save history each N steps if requested
128                    if self.savehist == True and step%N == 0:
129                        self.save_data(G, it, step, directory_name)
130                    #Save last 1000 steps
131                    if step >= S-1000:
132                        self.asymptotic_data(G, it, step, S, directory_name)
133        return G
134
135 def expA_grid(B = 0.5, XM = 0.5):
136     params = {'B' : [B], 'XM' : [XM], 'N' : [101], 'E' : [0.1], 'T' : [0.25], 'R' :
               [0.25], 'S' : [2000000]}
137     exp = ARM_MM(params, iters=20, seed=None, savehist=False)
138     exp.arm_MM()
139
140 if __name__ == "__main__":
141     #Number of laptop CPUs to be used
142     n_cpu = mp.cpu_count()
143     # Call Pool
144     pool = mp.Pool(processes=n_cpu)
145     # Define ranges of XM and B values
146     B_range = np.arange(0, 1.0 + 1/50, 1/50)
147     XM_range = np.arange(0, 1.0 + 1/50, 1/50)
148     # Create a list of tuples containing all combinations of XM and B values
149     param_tuples = [(B, XM) for B in B_range for XM in XM_range]
150     # Call expC_grid for all parameter tuples using pool.map
151     results = pool.starmap(expA_grid, param_tuples)
152     # Close the pool
153     pool.close()
```

Appendix B

Computer code for the Coevolutionary Attraction-Repulsion Model

In this Appendix, we share our code for the simulation of the Coevolutionary Attraction-Repulsion Model. This code was developed in Python by using the library NetworkX. The program can save the network data for the entire simulation history or only in the asymptotic state, stored in a folder called "networks." The networks are saved using the pickle library. When saving the complete history, the networks will be generated at intervals of every N steps until the system reaches either a convergence state or the maximum time steps limit. When only the asymptotic state is needed, the program will save only the last network if the system reaches convergence. Otherwise, it will save the last one thousand networks before reaching the time steps limit. To obtain estimates of computational time, you can enable time measurement by modifying the `trange` function as follows: `disable=False`. All our statistical calculations were performed using these output files.

In the final section, the script includes the experiment `expA_Pr_T`, which generates data for asymptotic states across a range of P_r values for different T values over fifty iterations. The code is parallelized using the multiprocessing library.

A more comprehensive version of the code that includes the statistical analysis with the respective instructions can be found in the GitHub repository **https://github.com/mateocarpio/Coevolutionary-ARM**.

```python
#!/usr/bin/env python

#import libraries
import networkx as nx
import numpy as np
from tqdm import trange
import math
```

```python
8   from itertools import product
9   import os
10  import pickle
11  import multiprocessing as mp
12
13  class ARM_Coevolution():
14      def __init__(self, params, iters, seed, savehist=True):
15          defaults = {'N' : [100], 'E' : [0.1], 'T' : [0.25], 'R' : [0.25], 'S' :
                [500000], 'Pr' : [0.5]}
16          plist = [params[p] if p in params else defaults[p] for p in defaults]
17          self.params = list(product(*plist))
18          self.iters = iters
19          self.rng = np.random.default_rng(seed)
20          self.savehist = savehist
21          self.directory_name = "Pr_{:.5f}-T_{:.2f}".format(round(plist[5][0], 5),
                round(plist[2][0], 2))
22
23      #Create intial opinions
24      def initializing(self, N):
25          config = np.zeros(N)
26          for i in np.arange(N):
27          #initial opinions follows a Gaussian distribution
28              while True:
29                  config[i] = self.rng.normal(0.5, 0.2)
30                  if 0 <= config[i] and config[i] <= 1:
31                      break
32          config = config.reshape(-1, 1)
33          init_config = config
34          return config
35
36      #Create the random network
37      def random_network(self, N, config):
38          G = nx.random_regular_graph(4, N)
39          for i in G.nodes:
40                  G.add_nodes_from([i], opinion=config[i])
41          return G
42
43      #Save the network
44      def save_network(self, G, step, directory, it):
45          if not os.path.exists("./outputfolder/"+str(directory)+"/networks"):
46              os.makedirs("./outputfolder/" + str(directory)+"/networks")
```

```python
47          with open(f"./outputfolder/{directory}/networks/net_iter-{it}_step-{step}",
                'wb') as f:
48              pickle.dump(G, f)
49
50      #Save the asymptotics networks
51      def save_asymp_network(self, G, step, directory, it):
52          if not os.path.exists("./outputfolder/"+str(directory)+"/networks"):
53              os.makedirs("./outputfolder/" + str(directory)+"/networks")
54          with
                open(f"./outputfolder/{directory}/networks/asympNet_iter-{it}_step-{step}",
                'wb') as f:
55              pickle.dump(G, f)
56
57      #stop conditon
58      def test_if_can_stop(self, G, vars):
59          opinions = nx.get_node_attributes(G, "opinion").values()
60          variance = np.var(list(opinions))
61          vars.append(variance)
62          _res = False
63          _reason = None
64          counter = 0
65          if len(vars) > 100:
66              for i in range(100):
67                  if abs(vars[-1] - vars[-(i+1)]) < 10**(-6):
68                      counter +=1
69              if counter == 100:
70                  _res = True
71                  _reason = 'No variance change'
72          return _res, _reason, vars
73
74      #Dynamics based on the attraction-repulsion rule
75      def node_dynamics(self, G, i, T, R, E):
76          if len(G[i])>0:
77              j = self.rng.choice(G[i]) #choose a random neighbor
78              dist = (abs(G.nodes[i]["opinion"] - G.nodes[j]["opinion"])) #calcualte
                    distance between opinions
79              prob = math.pow(0.5, dist/E)
80              if self.rng.random() <= prob:
81                  if dist <= T: #condition for atrarction d < T
82                      #i get closer to j R times their distance
83                      G.nodes[i]["opinion"] = G.nodes[i]["opinion"] + R *
```

```python
                       (G.nodes[j]["opinion"] - G.nodes[i]["opinion"])
               else: #condition for repulsion d > T
                   G.nodes[i]["opinion"] = G.nodes[i]["opinion"] - R * \
                       (G.nodes[j]["opinion"] - G.nodes[i]["opinion"])
               G.nodes[i]["opinion"] = np.maximum(0,
                   np.minimum(1,G.nodes[i]["opinion"])) #set limits [0-1]
        return G


    #Disconnect of any neighbor
    def disconect(self, G, i, T):
        condition = False
        choices = []
        #To prevent isolated nodes
        for k in G[i]:
          if len(G[k])>1:
            choices.append(k)
        if len(choices) > 0:
            j = self.rng.choice(choices)
            G.remove_edge(i,j)
            condition = True
        return G, condition


    #Connect to a neighbor that is incide the confidence bound
    def rewiring(self, G, i, T):
      # To control if there is possible the rewiring
        condition = False
        possible_choices = list(set(G.nodes) - set(G.neighbors(i)) - set({i})) #No
            neighbors
        set_choice = []
        #Select neighbors between the tolerance T
        for k in possible_choices:
            if abs(G.nodes[i]["opinion"] - G.nodes[k]["opinion"]) < T:
                set_choice.append(k)
        if len(set_choice) > 0:
            condition = True
            l = self.rng.choice(set_choice)
            G.add_edge(i, l)
        return condition, G


    def perform_time_step(self, G, T, R, E, pr):
        i = self.rng.choice(G.nodes) #choose a random node
```

```python
121              if self.rng.random() <= pr:
122                  condition_1, G = self.rewiring(G, i, T)
123                  if condition_1 == True:
124                      G, condition_2 = self.disconect(G, i, T)
125                      if condition_2 == False:
126                          G.remove_edge(i, l)
127              else:
128                  G = self.node_dynamics(G, i, T, R, E)
129              return G
130
131      def arm_coe(self):
132          for param in self.params:
133              print(param)
134              N, E, T, R, S, Pr = param
135              directory_name = "Pr_{:.5f}-T_{:.2f}".format(round(Pr, 5), round(T, 2))
136              if not os.path.exists("./outputfolder/"+str(directory_name)):
137                  os.makedirs("./outputfolder/" + str(directory_name))
138              for it in range(self.iters):
139                  config = self.initializing(N)
140                  G = self.random_network(N, config)
141                  pos = nx.spring_layout(G, scale=2, seed=213123)
142                  vars = []
143                  _res = False
144                  inner_loop_terminated = False
145                  for step in trange(S, desc='Simulating interactions', disable=False):
146                      G = self.perform_time_step(G, T, R, E, Pr)
147                      if step%N==0:
148                          if self.savehist == True:
149                              self.save_network( G, step, directory_name, it)
150                      #evaluete the stop condition
151                          _res, _reason, vars = self.test_if_can_stop(G, vars)
152                          if _res == True:
153                                  self.save_asymp_network(G, step, directory_name, it)
154                                  inner_loop_terminated = True
155                                  self.save_asymp_network(G, step, directory_name, it)
156                                  break
157                      #save the last 1000 steps
158                      if step >= S-1000:
159                          self.save_asymp_network(G, step, directory_name, it)
160          return G, step
161
```

```python
162
163  def expA_Pr_T(Pr=0.1, T=0.25):
164      params = {'N' : [100], 'E' : [0.1], 'T' : [T], 'R' : [0.25], 'S' : [2000001],
                   'Pr' : [Pr]}
165      exp = ARM_Coevolution(params, iters=50, seed=None, savehist=False)
166      exp.arm_coe()
167
168  if __name__ == "__main__":
169      #Number of laptop CPUs to be used
170      n_cpu = 1
171      # Call Pool
172      pool = mp.Pool(processes=n_cpu)
173      # Define ranges of XM and B values
174      Pr_range = np.logspace(np.log10(0.0001), np.log10(0.9), num=100)
175      T_range = [0.20,0.25]
176      # Create a list of tuples containing all combinations of XM and B values
177      param_tuples = [(Pr, T) for Pr in Pr_range for T in T_range]
178      # Call expC_grid for all parameter tuples using pool.map
179      results = pool.starmap(expA_Pr_T, param_tuples)
180      # Close the pool
181      pool.close()
```

Bibliography

[1] Schweitzer, F.; Farmer, J. D. *Brownian agents and active particles: collective dynamics in the natural and social sciences*; Springer, 2003; Vol. 1.

[2] Holland, J. H. *Complexity: A very short introduction*; OUP Oxford, 2014.

[3] Fieguth, P. *Introduction to Complex Systems*; Springer, 2021.

[4] Sayama, H. *Introduction to the modeling and analysis of complex systems*; Open SUNY Textbooks, 2015.

[5] Weisbuch, G. Social opinion dynamics. *Econophysics and Sociophysics: Trends and Perspectives* **2006**, 67–94.

[6] Castellano, C.; Fortunato, S.; Loreto, V. Statistical physics of social dynamics. *Reviews of modern physics* **2009**, *81*, 591.

[7] Baronchelli, A. The emergence of consensus: a primer. *Royal Society open science* **2018**, *5*, 172189.

[8] Sawyer, R. K. *Social emergence: Societies as complex systems*; Cambridge University Press, 2005; Chapter 8 Simulating social emergence with artificial societies.

[9] Barrera Lemarchand, F.; Semeshenko, V.; Navajas, J.; Balenzuela, P. Polarizing crowds: Consensus and bipolarization in a persuasive arguments model. *Chaos: An Interdisciplinary Journal of Nonlinear Science* **2020**, *30*, 063141.

[10] Hohmann, M.; Devriendt, K.; Coscia, M. Quantifying ideological polarization on a network using generalized Euclidean distance. *Science Advances* **2023**, *9*, eabq2044.

[11] Cota, W.; Ferreira, S. C.; Pastor-Satorras, R.; Starnini, M. Quantifying echo chamber effects in information spreading over political communication networks. *EPJ Data Science* **2019**, *8*, 35.

[12] Quattrociocchi, W.; Scala, A.; Sunstein, C. R. Echo chambers on Facebook. *Available at SSRN 2795110* **2016**,

[13] McCoy, J.; Rahman, T.; Somer, M. Polarization and the global crisis of democracy: Common patterns, dynamics, and pernicious consequences for democratic polities. *American Behavioral Scientist* **2018**, *62*, 16–42.

[14] Handlin, S. The logic of polarizing populism: State crises and polarization in South America. *American Behavioral Scientist* **2018**, *62*, 75–91.

[15] Axelrod, R.; Daymude, J. J.; Forrest, S. Preventing extreme polarization of political attitudes. *Proceedings of the National Academy of Sciences* **2021**, *118*, e2102139118.

[16] Wilensky, U.; Rand, W. *An introduction to agent-based modeling: modeling natural, social, and engineered complex systems with NetLogo*; Mit Press, 2015.

[17] Axelrod, R. *Simulating social phenomena*; Springer, 1997; pp 21–40.

[18] Wilensky, U.; Papert, S. Restructurations: Reformulations of knowledge disciplines through new representational forms. *Constructionism* **2010**, *17*, 1–15.

[19] Epstein, J. M.; Axtell, R. *Growing artificial societies: social science from the bottom up*; Brookings Institution Press, 1996.

[20] Newman, M. *Networks*; Oxford university press, 2018.

[21] Erdos, P.; Rényi, A. On random graphs I. *Publ. math. debrecen* **1959**, *6*, 18.

[22] Watts, D. J.; Strogatz, S. H. Collective dynamics of 'small-world'networks. *nature* **1998**, *393*, 440–442.

[23] Xia, H.; Wang, H.; Xuan, Z. Opinion dynamics: A multidisciplinary review and perspective on future research. *International Journal of Knowledge and Systems Science (IJKSS)* **2011**, *2*, 72–91.

[24] Bikhchandani, S.; Hirshleifer, D.; Welch, I. A theory of fads, fashion, custom, and cultural change as informational cascades. *Journal of political Economy* **1992**, *100*, 992–1026.

[25] Wood, W. Attitude change: Persuasion and social influence. *Annual review of psychology* **2000**, *51*, 539–570.

[26] Byrne, D. Interpersonal attraction and attitude similarity. *The journal of abnormal and social psychology* **1961**, *62*, 713.

[27] Clifford, P.; Sudbury, A. A model for spatial conflict. *Biometrika* **1973**, *60*, 581–588.

[28] Dornic, I.; Chaté, H.; Chave, J.; Hinrichsen, H. Critical coarsening without surface tension: The universality class of the voter model. *Physical Review Letters* **2001**, *87*, 045701.

[29] Castelló, X.; Toivonen, R.; Eguíluz, V. M.; Saramäki, J.; Kaski, K.; San Miguel, M. Anomalous lifetime distributions and topological traps in ordering dynamics. *Europhysics Letters* **2007**, *79*, 66006.

[30] Holme, P.; Newman, M. E. Nonequilibrium phase transition in the coevolution of networks and opinions. *Physical Review E* **2006**, *74*, 056108.

[31] Deffuant, G.; Amblard, F.; Weisbuch, G.; Faure, T. How can extremism prevail? A study based on the relative agreement interaction model. *Journal of artificial societies and social simulation* **2002**, *5*.

[32] Axelrod, R. The dissemination of culture: A model with local convergence and global polarization. *Journal of conflict resolution* **1997**, *41*, 203–226.

[33] DeGroot, M. H. Reaching a consensus. *Journal of the American Statistical association* **1974**, *69*, 118–121.

[34] Deffuant, G.; Neau, D.; Amblard, F.; Weisbuch, G. Mixing beliefs among interacting agents. *Advances in Complex Systems* **2000**, *3*, 87–98.

[35] Baldassarri, D.; Bearman, P. Dynamics of political polarization. *American sociological review* **2007**, *72*, 784–811.

[36] Krause, S. M.; Weyhausen-Brinkmann, F.; Bornholdt, S. Repulsion in controversial debate drives public opinion into fifty-fifty stalemate. *Physical Review E* **2019**, *100*, 042307.

[37] Bail, C. A.; Argyle, L. P.; Brown, T. W.; Bumpus, J. P.; Chen, H.; Hunzaker, M. F.; Lee, J.; Mann, M.; Merhout, F.; Volfovsky, A. Exposure to opposing views on social media can increase political polarization. *Proceedings of the National Academy of Sciences* **2018**, *115*, 9216–9221.

[38] Yang, V. C.; Abrams, D. M.; Kernell, G.; Motter, A. E. Why are US parties so polarized? A "satisficing" dynamical model. *SIAM Review* **2020**, *62*, 646–657.

[39] Schaffner, B.; Ansolabehere, S.; Luks, S. Cooperative election study common content, 2020. *Harvard Dataverse* **2021**, *1*.

[40] Carletti, T.; Fanelli, D.; Grolli, S.; Guarino, A. How to make an efficient propaganda. *Europhysics Letters* **2006**, *74*, 222.

[41] Levendusky, M. S. Why do partisan media polarize viewers? *American journal of political science* **2013**, *57*, 611–623.

[42] Lupu, N. Party polarization and mass partisanship: A comparative perspective. *Political Behavior* **2015**, *37*, 331–356.

[43] González-Avella, J. C.; Cosenza, M. G.; Tucci, K. Nonequilibrium transition induced by mass media in a model for social influence. *Physical Review E* **2005**, *72*, 065102.

[44] González-Avella, J. C.; Eguíluz, V. M.; Cosenza, M. G.; Klemm, K.; Herrera, J. L.; San Miguel, M. Local versus global interactions in nonequilibrium transitions: A model of social dynamics. *Physical Review E* **2006**, *73*, 046119.

[45] González-Avella, J. C.; Cosenza, M. G.; Eguíluz, V. M.; San Miguel, M. Spontaneous ordering against an external field in non-equilibrium systems. *New Journal of Physics* **2010**, *12*, 013010.

[46] Martins, T. V.; Pineda, M.; Toral, R. Mass media and repulsive interactions in continuous-opinion dynamics. *Europhysics Letters* **2010**, *91*, 48003.

[47] Gross, T.; Blasius, B. Adaptive coevolutionary networks: a review. *Journal of the Royal Society Interface* **2008**, *5*, 259–271.

[48] Gross, T.; Sayama, H. *Adaptive networks*; Springer, 2009.

[49] Herrera, J. L.; Cosenza, M. G.; Tucci, K.; González-Avella, J. C. General coevolution of topology and dynamics in networks. *Europhysics Letters* **2011**, *95*, 58006.

[50] Min, B.; Miguel, M. S. Fragmentation transitions in a coevolving nonlinear voter model. *Scientific reports* **2017**, *7*, 12864.

[51] Kozma, B.; Barrat, A. Consensus formation on adaptive networks. *Physical Review E* **2008**, *77*, 016102.

[52] Stauffer, D.; Hohnisch, M.; Pittnauer, S. The coevolution of individual economic characteristics and socioeconomic networks. *Physica A: Statistical Mechanics and its Applications* **2006**, *370*, 734–740.

[53] Robertson, R. E.; Green, J.; Ruck, D. J.; Ognyanova, K.; Wilson, C.; Lazer, D. Users choose to engage with more partisan news than they are exposed to on Google Search. *Nature* **2023**, 1–7.

[54] Garrett, R. K. Echo chambers online?: Politically motivated selective exposure among Internet news users. *Journal of computer-mediated communication* **2009**, *14*, 265–285.

[55] Currin, C. B.; Vera, S. V.; Khaledi-Nasab, A. Depolarization of echo chambers by random dynamical nudge. *Scientific Reports* **2022**, *12*, 9234.

[56] Cinus, F.; Minici, M.; Monti, C.; Bonchi, F. The effect of people recommenders on echo chambers and polarization. **2022**, *16*, 90–101.